Latin American Journal of Solids and Structures
www.lajss.org

Research on Free Vibration Frequency Characteristics of Rotating Functionally Graded Material Truncated Conical Shells with Eccentric Functionally Graded Material Stringer and Ring Stiffeners

Abstract

In this research work, an exact analytical solution for frequency characteristics of the free vibration of rotating functionally graded material (FGM) truncated conical shells reinforced by eccentric FGM stringers and rings has been investigated by the displacement function method. Material properties of shell and stiffeners are assumed to be graded in the thickness direction according to a simple power law distribution. The change of spacing between stringers is considered. Using the Donnell shell theory, Leckhnisky smeared stiffeners technique and taking into account the influences of centrifugal force and Coriolis acceleration the governing equations are derived. For stiffened FGM conical shells, it is difficult that free vibration equations are a couple set of three *variable coefficient* partial differential equations. By suitable transformations and applying Galerkin method, this difficulty is overcome in the paper. The sixth order polynomial equation for ω is obtained and it is used to analyze the frequency characteristics of rotating ES-FGM conical shells. Effects of stiffener, geometrics parameters, cone angle, vibration modes and rotating speed on frequency characteristics of the shell forward and backward wave are discussed in detail. The present approach proves to be reliable and accurate by comparing with published results available in the literature.

Keywords

Rotating truncated conical shell; Free vibration; Frequency characteristics; FGM stiffener; Functionally graded material (FGM).

Dao Van Dung [a]
Hoang Thi Thiem [a, *]

[a] Vietnam National University, Hanoi, Viet Nam

Corresponding author:
[*] hoangthithiem13@gmail.com

http://dx.doi.org/10.1590/1679-78252886

Received 25.02.2016
In revised form 18.07.2016
Accepted 02.08.2016
Available online 03.08.2016

1 INTRODUCTION

Revolution shell structures involving functionally graded material (FGM) conical shells potentially have wide application in many modern industry fields such as aerospace, airplane, missile, booster

and other aerospace vehicles (Koizumi M. 1993, Shen HS. 2009). Therefore, the free vibration of rotating truncated conical shells is one of interesting and important problems and has received considerable attention of researchers.

For unstiffened conical shells, much significant results are obtained. Chandrasekharan and Ramamurti (1981 and 1982) studied axisymmetric and asymmetric free vibrations of laminated conical shells using the Rayleigh-Ritz procedure. Shu (1996) presented an efficient approach for analyzing the free vibration of conical shells. The same author (1996) investigated the free vibration of composite laminated conical shells by generalized differential quadrature. By using the Galerkin and harmonic balance methods, Xu et al. (1996) studied the nonlinear free vibration of a symmetrically laminated, cross-ply, geometrically perfect thick conical shell with its two ends both clamped and both simply supported. Lam and Hua (1997 and 1999) analyzed the vibration and influences of boundary conditions on the frequency characteristics of rotating truncated circular conical shells. Following this direction, the frequency analysis of rotating truncated circular orthotropic conical shells with different boundary conditions was studied by Hua (2000). That same author (2000), based on the Love first approximation theory and Galerkin procedure, and taking into account the influences of centrifugal and Coriolis accelerations, investigated frequency characteristics of a rotating truncated circular layered conical shell. With the improved generalized differential quadrature method, Lam et al. (2002) analyzed free vibration characteristics of truncated conical panels. Using the classical thin shell theory and the element-Free kp-Ritz method, Liew et al. (2005) investigated the free vibration of thin conical shells. Civalek (2006) proposed the discrete singular convolution method for analyzing the free vibration of rotating conical shells in which a regularized Shannon's delta kernel is selected as the singular convolution to illustrate his algorithm. Sofiyev et al. (2010), by using the Donnell shell theory and Galerkin method, presented an analytical procedure to study the free vibration and stability of homogeneous and non-homogeneous orthotropic truncated and complete conical shells with clamped edges under external pressure.

For unstiffened FGM conical shells, there are many available results. Tornabene (2009) and Tornabene et al. (2009), based on the first order shear deformation theory and 2-D differential quadrature solution, studied the free vibration analysis of functionally graded conical, cylindrical and annular plates structures using 2-D differential quadrature solution. Sofiyev (2009) analyzed the vibration and stability behavior of freely supported FGM conical shells subjected to external pressure by Galerkin method. The same author (2012) analyzed the nonlinear vibration of FGM truncated conical shells by analytical approach. For unstiffened FGM conical panels, Bich et al. (2012) investigated by analytical method the linear mechanical buckling of that structure using the classical shell theory and Galerkin method. The investigation on the linear buckling of truncated hybrid FGM conical shells with piezoelectric layers subjected to combined action of thermal and electrical loads was reported by Torabi et al. (2013). Based on the First order shear deformation theory (FSDT), Malekzadeh and Heydarpour (2013) studied effects of centrifugal and Coriolis, of geometrical and material parameters on the free vibration behavior of rotating FGM un-stiffened truncated conical shells subjected to different boundary conditions.

As can be seen the above introduced results only relate to unstiffened structures. However, in practice, plates and shells including conical shells usually are reinforced by stiffeners system to provide the benefit of added load carrying capability with a relatively small additional

weight. Thus, the study on dynamic behavior of those structures is significant practical problem.

For stiffened isotropic or orthotropic conical shells, Weingarten (1965) studied the free vibration of a ring-stiffened simply supported conical shell by considering an equivalent orthotropic shell and using Galerkin method. Applying the energy approach, Crenwelge and Muster (1969) investigated the resonant frequencies of simply supported ring-stiffened, and ring and stringer-stiffened conical shells. Rao and Reddy (1981) studied the minimum weight design of axially loaded simply supported stiffened conical shells with natural frequency constraints. The influence of placing the stiffeners inside as well as outside the conical shell on the optimum design is considered. The expressions for the critical axial buckling load and natural frequency of vibration of conical shell also are obtained. By applying structural symmetry techniques, Mustaffa and Ali (1987) investigated free vibration characteristics of stiffened cylindrical and conical shells. Srinivasan and Krishnan (1989), using the integral equation for the space domain and mode superposition for the time domain, obtained the results on the dynamic response analysis of stiffened conical shell panels in which the effect of eccentricity is taken into account. Mecitoglu (1996) studied the vibration characteristics of stiffened truncated conical shells based on the Donnell-Mushtari thin shell theory, the stiffeners smeared technique and the collocation method. The problem on the free vibration of rotating composite conical shells with stringer and ring stiffeners was solved by Talebitooti et al. (2010).

For stiffened FGM shells, Najafizadeh et al. (2009) with the linearized stability equations in terms of displacements studied buckling of FGM cylindrical shell reinforced by rings and stringers under axial compression. The stiffeners and skin, in their work, are assumed to be made of functionally graded materials and its properties vary continuously through the thickness direction. Following this direction, Dung and Hoa (2015) obtained the results on the static nonlinear buckling and post-buckling analysis of eccentrically stiffened FGM circular cylindrical shells under torsional loads in thermal environment. The material properties of shell and stiffeners are assumed to be continuously graded in the thickness direction. Galerkin method was used to obtain closed-form expressions to determine critical buckling loads. Dung et al. (2014) investigated the static buckling of FGM conical shells reinforced by FGM stiffeners under axial compressive load and external pressure by analytical method. The change of distance between stringers is considered in that work. By considering homogenous stiffeners, Bich et al. (2013) obtained the results on the nonlinear static and dynamic analysis of eccentrically stiffened FGM cylindrical shells and doubly curved thin shallow shells based on the classical shell theory. The governing equations of motion were derived by using the smeared stiffeners technique and the classical shell theory with von Karman geometrical nonlinearity. The nonlinear critical dynamic buckling load is found according to the Budiansky-Roth criterion. Dung et al. (2013) studied a mechanical buckling of eccentrically stiffened functionally graded (ES-FGM) thin truncated conical shells subjected to axial compressive load and uniform external pressure load based on the smeared stiffeners technique and the classical shell theory and considering homogenous stiffeners. Dung and Nam (2014) solved the problem on the nonlinear dynamic analysis of eccentrically stiffened functionally graded circular cylindrical thin shells under external pressure and surrounded by an elastic medium. The nonlinear critical dynamic buckling load is found according to the Budiansky-Roth criterion.

From the review of the literature, as can be seen the free vibration of rotating FGM truncated conical shell reinforced by eccentric stiffener system and taking into account the influences of centrifugal force and Coriolis acceleration still is not investigated. The aim of this paper is to investigate just mentioned problem. We focus on three new contributions as: FGM truncated conical shells are reinforced by FGM stringers and rings; A change of spacing between stringer stiffeners is considered; A centrifugal force and Coriolis acceleration are taken into account. The governing equations are derived using Donnell shells theory and smeared stiffeners technique. For stiffened FGM conical shells, it is difficult that these equations are a couple set of three *variable coefficient* partial differential equations, while for stiffened cylindrical shells those governing equations only are a couple set of *constant coefficient* partial differential equations. This difficulty is overcome in the paper. The sixth order polynomial equation for frequency ω is obtained by applying Galerkin method. Numerical simulations are been done to show effects of geometrics parameters, vibration modes and rotating speed, reinforcement stiffener on frequency characteristics of the shell. The present results are validated by comparing with those in the literature.

2 MATERIAL PROPERTIES OF SHELL AND STIFFENERS

Consider a thin circular truncated conical shell with the semi-vertex angle a, thickness h, length L and small base radius r as shown in Fig. 1. The curvilinear coordinate system is defined as $\left(x, \theta, z\right)$, where the origin is located in the middle surface of the shell, x is in the generatrix direction measured from the vertex of shell, θ is in the circumferential direction and the axes z is perpendicular to the plane $\left(x, \theta\right)$ and its direction is the outwards normal direction of the conical shell. Denotes x_0 - the distance from the vertex to small base, and u, v and w - the displacement components of a point in the middle surface in the direction x, θ and z, respectively.

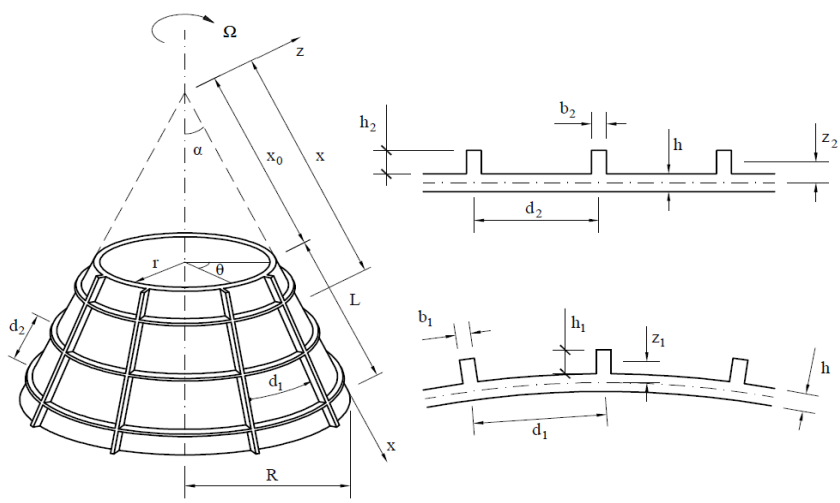

Figure 1: Geometry and coordinate system of a stiffened FGM truncated conical.

Assume that the FGM conical shell rotates about its vertical symmetrical axis with a constant angular velocity denoted by Ω. Also assume that the shell is stiffened by closely spaced circular rings and longitudinal stringers and the stiffeners and skin are made of functionally graded materials varying continuously through the thickness direction of the shell with the power law. Two cases are investigated in this work.

Case 1: Conical shell with ceramic outside surface and metal inside surface and inside stiffener.

Case 2: Conical shell with ceramic outside surface and metal inside surface and outside stiffener.

For case 1, Young Modulus and densities of FGM shell and FGM stiffeners are given by (Najafizadeh et al., 2009; Dung et al., 2014)

$$E_{sh} = E_m + E_{cm}\left(\frac{2z+h}{2h}\right)^k, -h/2 \le z \le h/2, k \ge 0; \tag{1}$$

$$\rho_{sh} = \rho_m + \rho_{cm}\left(\frac{2z+h}{2h}\right)^k, -h/2 \le z \le h/2, k \ge 0; \tag{2}$$

$$E_s = E_m + E_{cm}\left(-\frac{2z+h}{2h_1}\right)^{k_2}, -h/2-h_1 \le z \le -h/2, k_2 \ge 0; \tag{3}$$

$$\rho_s = \rho_m + \rho_{cm}\left(-\frac{2z+h}{2h_1}\right)^{k_2}, -h/2-h_1 \le z \le -h/2, k_2 \ge 0; \tag{4}$$

$$E_r = E_m + E_{cm}\left(-\frac{2z+h}{2h_2}\right)^{k_3}, -h/2-h_2 \le z \le -h/2, k_3 \ge 0; \tag{5}$$

$$\rho_r = \rho_m + \rho_{cm}\left(-\frac{2z+h}{2h_2}\right)^{k_3}, -h/2-h_2 \le z \le -h/2, k_3 \ge 0. \tag{6}$$

where $\nu_{sh} = \nu_s = \nu_r = \nu = const$, k, k_2 and k_3 are volume fractions indexes of shell, stringer and ring, respectively and subscripts *c, m, sh, s* and *r* denote ceramic, metal, shell, longitudinal stringers and circular ring, respectively. It is evident that, from Eqs. (1)-(6), a continuity between the shell and stiffeners is satisfied. Note that the thickness of the stringer and the ring are respectively denoted by h_1, and h_2; and E_c, E_m are Young Modulus of the ceramic and metal; and E_{sh}, E_s, E_r, ρ_{sh}, ρ_s, ρ_r are Young Modulus and densities of shell, of stiffener in the *x*-direction and θ-direction, respectively. The coefficient ν is Poison's ratio.

Note $k_2 = k_3 = k$, when $k_2 \to \infty, k_3 \to \infty$ leads to homogeneous stiffener.

The Poisson's ratio ν is assumed to be constant.

Young Modulus and densities for the case 2 are given in Appendix I.

3 FUNDAMENTAL EQUATIONS

According to the Donnell shell theory, the strain components at distance z from the reference surface of shell are of the form (Brush and Almroth, 1975; Reddy, 2004; Volmir, 1972)

$$\begin{bmatrix}\varepsilon_x\\ \varepsilon_\theta\\ \gamma_{x\theta}\end{bmatrix}=\begin{bmatrix}\varepsilon_{xm}\\ \varepsilon_{\theta m}\\ \gamma_{x\theta m}\end{bmatrix}+z\begin{bmatrix}k_x\\ k_\theta\\ 2k_{x\theta}\end{bmatrix}; \tag{7}$$

where ε_{xm} and $\varepsilon_{\theta m}$ are the middle surface strains in meridional and circumferential direction, and $\gamma_{x\theta m}$ is the shear strain of the middle surface of the shell, and k_x, k_θ and $k_{x\theta}$ are the change of curvatures and twist, respectively. They are related to the displacement components u,v,w as (Brush and Almroth, 1975; Volmir, 1972; Hua, 2000)

$$\begin{bmatrix}\varepsilon_{xm}\\ \varepsilon_{\theta m}\\ \gamma_{x\theta m}\end{bmatrix}=\begin{bmatrix}u_{,x}\\ \dfrac{1}{x\sin\alpha}\mathrm{v}_{,\theta}+\dfrac{u}{x}+\dfrac{w}{x}\cot\alpha\\ \dfrac{1}{x\sin\alpha}u_{,\theta}-\dfrac{\mathrm{v}}{x}+\mathrm{v}_{,x}\end{bmatrix};$$

$$\begin{bmatrix}k_x\\ k_\theta\\ k_{x\theta}\end{bmatrix}=\begin{bmatrix}-w_{,xx}\\ -\dfrac{1}{x^2\sin^2\alpha}w_{,\theta\theta}+\dfrac{\cos\alpha}{x^2\sin^2\alpha}v_{,\theta}-\dfrac{w_{,x}}{x}\\ -\dfrac{1}{x\sin\alpha}w_{,x\theta}+\dfrac{1}{x^2\sin\alpha}w_{,\theta}+\dfrac{\cos\alpha}{x\sin\alpha}v_{,x}-\dfrac{\cos\alpha}{x^2\sin\alpha}v\end{bmatrix}. \tag{8}$$

Using Hooke's Law, the stress-strain relations are expressed by:
For the conical shell

$$\begin{bmatrix}\sigma_x^{sh}\\ \sigma_\theta^{sh}\\ \sigma_{x\theta}^{sh}\end{bmatrix}=\begin{bmatrix}\dfrac{E_{sh}}{1-\nu^2}\left(\varepsilon_x+\nu\varepsilon_\theta\right)\\ \dfrac{E_{sh}}{1-\nu^2}\left(\varepsilon_\theta+\nu\varepsilon_x\right)\\ \dfrac{E_{sh}}{2\left(1+\nu\right)}\gamma_{x\theta}\end{bmatrix}. \tag{9}$$

For the stringer and ring stiffeners

$$\begin{bmatrix}\sigma_x^{st}\\ \sigma_\theta^{rt}\end{bmatrix}=\begin{bmatrix}E_s\varepsilon_x\\ E_r\varepsilon_\theta\end{bmatrix}; \tag{10}$$

where the subscripts *sh* and *st* denote shell and stiffeners, respectively, and E_s, E_r are Young Modulus of stringer and ring stiffener respectively.

The contribution of stiffeners is taken into account by using the smeared stiffener technique. In addition, the change of spacing between stringers in the meridional direction also is considered. Integrating the above stress-strain equations and their moments through the thickness of the shell, the expressions for force and moment resultants of ES-FGM truncated conical shells are defined as (Brush and Almroth, 1975; Najafizadeh et al., 2009; Dung et al., 2014)

$$\begin{bmatrix} N_x \\ N_\theta \\ N_{x\theta} \end{bmatrix} = \begin{bmatrix} \left(A_{11} + \dfrac{E_{1s}b_1}{d_1}\right)\varepsilon_{xm} + A_{12}\varepsilon_{\theta m} + \left(B_{11} + \dfrac{C_1^0}{x}\right)k_x + B_{12}k_\theta \\ A_{12}\varepsilon_{xm} + \left(A_{22} + \dfrac{E_{1r}b_2}{d_2}\right)\varepsilon_{\theta m} + B_{12}k_x + (B_{22} + C_2)k_\theta \\ A_{66}\gamma_{x\theta m} + 2B_{66}k_{x\theta} \end{bmatrix}; \tag{11}$$

$$\begin{bmatrix} M_x \\ M_\theta \\ M_{x\theta} \end{bmatrix} = \begin{bmatrix} \left(B_{11} + \dfrac{C_1^0}{x}\right)\varepsilon_{xm} + B_{12}\varepsilon_{\theta m} + \left(D_{11} + \dfrac{E_{3s}b_1}{d_1}\right)k_x + D_{12}k_\theta \\ B_{12}\varepsilon_{xm} + (B_{22} + C_2)\varepsilon_{\theta m} + D_{12}k_x + \left(D_{22} + \dfrac{E_{3r}b_2}{d_2}\right)k_\theta \\ B_{66}\gamma_{x\theta m} + 2D_{66}k_{x\theta} \end{bmatrix}; \tag{12}$$

where $C_1^0,\ C_2, d_1, d_2, E_{1s}, E_{1r}, E_{3s}, E_{3r},\ A_{ij}, B_{ij}, D_{ij}$ can be found in Appendix I.

The fundamental equations for the vibration of rotating truncated conical shells, basing on the Donnell shell theory, are as (Hua, 2000; Chen et al., 1993)

$$\begin{aligned} &\frac{\partial N_x}{\partial x} + \frac{1}{x\sin\alpha}\frac{\partial N_{x\theta}}{\partial \theta} + \frac{N_\theta^o}{x^2\sin^2\alpha}\left(\frac{\partial^2 u}{\partial \theta^2} - x\cos\alpha\sin\alpha\frac{\partial w}{\partial x}\right) + \frac{1}{x}(N_x - N_\theta) \\ &\qquad + 2\rho_1\Omega\sin\alpha\frac{\partial v}{\partial t} - \rho_1\frac{\partial^2 u}{\partial t^2} = 0; \\ &\frac{\partial N_{x\theta}}{\partial x} + \frac{1}{x\sin\alpha}\frac{\partial N_\theta}{\partial \theta} + \frac{\cot\alpha}{x}\frac{\partial M_{x\theta}}{\partial x} + \frac{\cos\alpha}{x^2\sin^2\alpha}\frac{\partial M_\theta}{\partial \theta} \\ &+ \frac{N_\theta^o}{x^2\sin^2\alpha}\left(x\sin\alpha\frac{\partial^2 u}{\partial x\partial\theta} + \sin\alpha\frac{\partial u}{\partial \theta} + x\sin^2\alpha\frac{\partial v}{\partial x}\right) + \frac{2N_{x\theta}}{x} \\ &\qquad - 2\Omega\rho_1\left(\sin\alpha\frac{\partial u}{\partial t} + \cos\alpha\frac{\partial w}{\partial t}\right) - \rho_1\frac{\partial^2 v}{\partial t^2} = 0; \\ &\frac{\partial^2 M_x}{\partial x^2} + \frac{2}{x\sin\alpha}\frac{\partial^2 M_{x\theta}}{\partial\theta\partial x} + \frac{1}{x^2\sin^2\alpha}\frac{\partial^2 M_\theta}{\partial\theta^2} + \frac{2}{x}\frac{\partial M_x}{\partial x} - \frac{1}{x}\frac{\partial M_\theta}{\partial x} \\ &+ \frac{N_\theta^o}{x^2\sin^2\alpha}\left(\frac{\partial^2 w}{\partial\theta^2} - x\sin\alpha\cos\alpha\frac{\partial u}{\partial x}\right) + \frac{N_\theta^o}{x^2\sin^2\alpha}\left(w\cos^2\alpha + u\sin\alpha\cos\alpha\right) - \frac{\cot\alpha}{x}N_\theta \end{aligned} \tag{13}$$

$$+2\rho_1\Omega\cos\alpha\frac{\partial v}{\partial t}-\rho_1\frac{\partial^2 w}{\partial t^2}=0.$$

where ρ_1 can be found in Appendix I, and the quality N_θ^0 is defined as the initial hoop tension due to the centrifugal force effect and given by (Hua, 2000)

$$N_\theta^o=\rho_1\Omega^2x^2\sin^2\alpha. \tag{14}$$

Note that the system of equations (13) not only consists of three terms of relative accelerations $\partial^2u/\partial t^2$, $\partial^2v/\partial t^2$ and $\partial^2w/\partial t^2$ but also four terms of Coriolis accelerations $2\Omega\sin\alpha\partial v/\partial t$, $2\Omega\sin\alpha\partial u/\partial t$, $2\Omega\cos\alpha\partial w/\partial t$ and $2\Omega\cos\alpha\partial v/\partial t$.

Introducing Eqs. (7-10) into Eqs. (11-12), then substituting the resulting equations and Eq. (14) into Eq. (13), the vibration equations in terms of displacements for rotating ES-FGM truncated conical shell are obtained as

$$R_{11}(u)+R_{12}(v)+R_{13}(w)=0; \tag{15}$$

$$R_{21}(u)+R_{22}(v)+R_{23}(w)=0; \tag{16}$$

$$R_{31}(u)+R_{32}(v)+R_{33}(w)=0; \tag{17}$$

where R_{ij} are partial differential operators and defined as following

$$\begin{aligned}R_{11}=&\left(A_{11}+\frac{E_{1s}b_1}{\lambda_0 x}\right)\frac{\partial^2}{\partial x^2}+\left[\frac{1}{x^2\sin^2\alpha}A_{66}+\left(\rho_2+\frac{\rho_3}{x}\right)\Omega^2\right]\frac{\partial^2}{\partial\theta^2}\\&+\frac{A_{11}}{x}\frac{\partial}{\partial x}-\frac{1}{x^2}\left(A_{22}+\frac{E_{1r}b_2}{d_2}\right)-\left(\rho_2+\frac{\rho_3}{x}\right)\frac{\partial^2}{\partial t^2};\end{aligned} \tag{18}$$

$$\begin{aligned}R_{12}=&\left[\frac{1}{x\sin\alpha}(A_{12}+A_{66})+\frac{\cot\alpha}{x^2\sin\alpha}(B_{12}+2B_{66})\right]\frac{\partial^2}{\partial x\partial\theta}-\left[\frac{1}{x^2\sin\alpha}\left(A_{22}+\frac{E_{1r}b_2}{d_2}+A_{66}\right)\right.\\&\left.+\frac{\cot\alpha}{x^3\sin\alpha}(B_{12}+2B_{66}+B_{22}+C_2)\right]\frac{\partial}{\partial\theta}+2\left(\rho_2+\frac{\rho_3}{x}\right)\Omega\sin\alpha\frac{\partial}{\partial t};\end{aligned} \tag{19}$$

$$\begin{aligned}R_{13}=&-\left(B_{11}+\frac{C_1^0}{x}\right)\frac{\partial^3}{\partial x^3}-\frac{1}{x^2\sin^2\alpha}(B_{12}+2B_{66})\frac{\partial^3}{\partial x\partial\theta^2}-\frac{B_{11}}{x}\frac{\partial^2}{\partial x^2}+\frac{1}{x^3\sin^2\alpha}\\&\times(B_{12}+2B_{66}+B_{22}+C_2)\frac{\partial^2}{\partial\theta^2}+\left[\frac{1}{x}A_{12}\cot\alpha+\frac{1}{x^2}(B_{22}+C_2)-\left(\rho_2+\frac{\rho_3}{x}\right)\Omega^2x\cos\alpha\sin\alpha\right]\frac{\partial}{\partial x}\\&-\frac{1}{x^2}\left(A_{22}+\frac{E_{1r}b_2}{d_2}\right)\cot\alpha;\end{aligned} \tag{20}$$

$$R_{21} = \left[\frac{1}{x\sin\alpha}(A_{12}+A_{66}) + \frac{\cot\alpha}{x^2\sin\alpha}(B_{12}+B_{66}) + \left(\rho_2+\frac{\rho_3}{x}\right)\Omega^2 x\sin\alpha\right]\frac{\partial^2}{\partial x\partial\theta}$$
$$+\left[\frac{1}{x^2\sin\alpha}\left(A_{22}+\frac{E_{1r}b_2}{d_2}+A_{66}\right) + \frac{\cot\alpha}{x^3\sin\alpha}(B_{22}+C_2-B_{66}) + \left(\rho_2+\frac{\rho_3}{x}\right)\Omega^2\sin\alpha\right]\frac{\partial}{\partial\theta} \quad (21)$$
$$-2\left(\rho_2+\frac{\rho_3}{x}\right)\Omega\sin\alpha\frac{\partial}{\partial t};$$

$$R_{22} = \left[A_{66}+\frac{3}{x}B_{66}\cot\alpha+\frac{2}{x^2}D_{66}\cot^2\alpha\right]\frac{\partial^2}{\partial x^2} + \left[\frac{1}{x^2\sin^2\alpha}\left(A_{22}+\frac{E_{1r}b_2}{d_2}\right) + \frac{2\cot\alpha}{x^3\sin^2\alpha}(B_{22}+C_2)\right.$$
$$\left.+\frac{\cot^2\alpha}{x^4\sin^2\alpha}\left(D_{22}+\frac{E_{3r}b_2}{d_2}\right)\right]\frac{\partial^2}{\partial^2\theta} + \left[\frac{1}{x}A_{66} - \frac{\cot\alpha}{x^2}B_{66} - \frac{4\cot^2\alpha}{x^3}D_{66}\right. \quad (22)$$
$$\left.+\left(\rho_2+\frac{\rho_3}{x}\right)\Omega^2 x\sin^2\alpha\right]\frac{\partial}{\partial x} + \left[-\frac{1}{x^2}A_{66} + \frac{\cot\alpha}{x^3}B_{66} + \frac{4\cot^2\alpha}{x^4}D_{66}\right] - \left(\rho_2+\frac{\rho_3}{x}\right)\frac{\partial^2}{\partial t^2};$$

$$R_{23} = -\left[\frac{1}{x\sin\alpha}(B_{12}+2B_{66}) + \frac{\cot\alpha}{x^2\sin\alpha}(D_{12}+2D_{66})\right]\frac{\partial^3}{\partial x^2\partial\theta}$$
$$-\left[\frac{1}{x^3\sin^3\alpha}(B_{22}+C_2) + \frac{\cot\alpha}{x^4\sin^3\alpha}\left(D_{22}+\frac{E_{3r}b_2}{d_2}\right)\right]\frac{\partial^3}{\partial\theta^3}$$
$$+\left[-\frac{1}{x^2\sin\alpha}(B_{22}+C_2) + \frac{\cot\alpha}{x^3\sin\alpha}\left(4D_{66}-D_{22}-\frac{E_{3r}b_2}{d_2}\right)\right]\frac{\partial^2}{\partial x\partial\theta} \quad (23)$$
$$+\left[\frac{\cot\alpha}{x^2\sin\alpha}\left(A_{22}+\frac{E_{1r}b_2}{d_2}\right) - \frac{4\cot\alpha}{x^4\sin\alpha}D_{66} + \frac{\cot^2\alpha}{x^3\sin\alpha}(B_{22}+C_2)\right]\frac{\partial}{\partial\theta} - 2\left(\rho_2+\frac{\rho_3}{x}\right)\Omega\cos\alpha\frac{\partial}{\partial t};$$

$$R_{31} = \left(B_{11}+\frac{C_1^0}{x}\right)\frac{\partial^3}{\partial x^3} + \frac{2}{x}B_{11}\frac{\partial^2}{\partial x^2} + \frac{(B_{12}+2B_{66})}{x^2\sin^2\alpha}\frac{\partial^3}{\partial x\partial\theta^2}$$
$$+\frac{1}{x^3\sin^2\alpha}(B_{22}+C_2-2B_{66})\frac{\partial^2}{\partial\theta^2}$$
$$-\left[\frac{\cot\alpha}{x}A_{12} + \frac{1}{x^2}(B_{22}+C_2) + \left(\rho_2+\frac{\rho_3}{x}\right)\Omega^2 x\sin\alpha\cos\alpha\right]\frac{\partial}{\partial x} + \frac{1}{x^3}(B_{22}+C_2) \quad (24)$$
$$-\frac{\cot\alpha}{x^2}\left(A_{22}+\frac{E_{1r}b_2}{d_2}\right) + \left(\rho_2+\frac{\rho_3}{x}\right)\Omega^2\sin\alpha\cos\alpha;$$

$$R_{32} = \left[\frac{1}{x\sin\alpha}(B_{12}+2B_{66}) + \frac{\cot\alpha}{x^2\sin\alpha}(D_{12}+4D_{66})\right]\frac{\partial^3}{\partial x^2\partial\theta}$$
$$+\left[\frac{1}{x^3\sin^3\alpha}(B_{22}+C_2) + \frac{\cot\alpha}{x^4\sin^3\alpha}\left(D_{22}+\frac{E_{3r}b_2}{d_2}\right)\right]\frac{\partial^3}{\partial\theta^3} \quad (25)$$

$$-\left[\frac{\cot\alpha}{x^3\sin\alpha}\left(2(D_{12}+4D_{66})+D_{22}+\frac{E_{3r}b_2}{d_2}\right)+\frac{1}{x^2\sin\alpha}(B_{22}+C_2+2B_{66})\right]\frac{\partial^2}{\partial x\partial\theta}$$
$$+\left[\frac{2\cot\alpha}{x^4\sin\alpha}\left(D_{12}+4D_{66}+D_{22}+\frac{E_{3r}b_2}{d_2}\right)+\frac{(1-\cot^2\alpha)(B_{22}+C_2)+2B_{66}}{x^3\sin\alpha}-\frac{\cot\alpha}{x^2\sin\alpha}\right.$$
$$\left.\times\left(A_{22}+\frac{E_{1r}b_2}{d_2}\right)\right]\frac{\partial}{\partial\theta}+2\left(\rho_2+\frac{\rho_3}{x}\right)\Omega\cos\alpha\frac{\partial}{\partial t};$$

$$R_{33}=-\left(D_{11}+\frac{E_{3s}b_1}{\lambda_0 x}\right)\frac{\partial^4}{\partial x^4}-\frac{1}{x^4\sin^4\alpha}\left(D_{22}+\frac{E_{3r}b_2}{d_2}\right)\frac{\partial^4}{\partial\theta^4}-\frac{2}{x^2\sin^2\alpha}(D_{12}+2D_{66})\frac{\partial^4}{\partial x^2\partial\theta^2}$$
$$-\frac{2}{x}D_{11}\frac{\partial^3}{\partial x^3}+\frac{2}{x^3\sin^2\alpha}(D_{12}+4D_{66})\frac{\partial^3}{\partial x\partial\theta^2}+\left[\frac{2\cot\alpha}{x}B_{12}+\frac{1}{x^2}\left(D_{22}+\frac{E_{3r}b_2}{d_2}\right)\right]\frac{\partial^2}{\partial x^2}$$
$$+\left[\frac{2\cot\alpha}{x^3\sin^2\alpha}(B_{22}+C_2)-\frac{2}{x^4\sin^2\alpha}\left(D_{12}+4D_{66}+D_{22}+\frac{E_{3r}b_2}{d_2}\right)+\left(\rho_2+\frac{\rho_3}{x}\right)\Omega^2\right]\frac{\partial^2}{\partial\theta^2} \quad (26)$$
$$-\frac{1}{x^3}\left(D_{22}+\frac{E_{3r}b_2}{d_2}\right)\frac{\partial}{\partial x}+\left[\frac{\cot\alpha}{x^3}(B_{22}+C_2)-\frac{\cot^2\alpha}{x^2}\left(A_{22}+\frac{E_{1r}b_2}{d_2}\right)+\left(\rho_2+\frac{\rho_3}{x}\right)\Omega^2\cos^2\alpha\right]$$
$$-\left(\rho_2+\frac{\rho_3}{x}\right)\frac{\partial^2}{\partial t^2};$$

The system of Eqs. (15-17) is used to analyze the frequency characteristics of rotating ES-FGM truncated conical shells. It is difficult that these equations are a couple set of three variable coefficient partial differential equations. This is a main difference between the free vibration analyses of rotating conical shell and cylindrical shell. This is also a reason why the investigations on the vibration of a rotating ES-FGM conical shell are very limited. This difficulty will be got over below.

4 BOUNDARY CONDITIONS AND SOLUTION OF THE PROBLEM

Assuming that the stiffened FGM truncated conical shell is simply supported at both ends. Thus the boundary conditions are expressed in the following form

$$\mathrm{v}=w=0,\ N_x=0,M_x=0 \quad \text{at} \quad x=x_0,x=x_0+L. \quad (27)$$

The displacement components satisfying accurately the above mentioned geometric boundary conditions and the force boundary conditions in the average sense, may be chosen as

$$u=\Psi_1\cos\frac{m\pi(x-x_0)}{L}\cos(n\theta+\omega t);$$
$$v=\Psi_2\sin\frac{m\pi(x-x_0)}{L}\sin(n\theta+\omega t); \quad (28)$$
$$w=\Psi_3\sin\frac{m\pi(x-x_0)}{L}\cos(n\theta+\omega t);$$

where m is the number of half-waves along a generatrix and n is the number of circumferential full-waves, ω (rad/s) is the natural circular frequency of the rotating ES-FGM conical shell, and Ψ_1, Ψ_2 and Ψ_3 are un-known constants.

As above noted, it is difficult to use the trial function (28) and Eqs. (15-17) to obtain directly the polynomial equation of frequency. Therefore, a different procedure is proposed as follows. Because $x_0 \le x \le x_0 + L; 0 \le \theta \le 2\pi,$ so we can carry out following equivalent transformations. Firstly multiplying Eq. (15) by x^2 and Eqs. (16, 17) by x^3, then applying Galerkin method for the resulting equations, leads to

$$\begin{aligned}
&\int_0^{\frac{2\pi}{\omega}} \int_{x_0}^{x_0+L} \int_0^{2\pi} x^3 \left[R_{11}(u) + R_{12}(v) + R_{13}(w)\right] \cos\frac{m\pi(x - x_0)}{L} \cos(n\theta + \omega t) \sin\alpha d\theta dx dt = 0;\\
&\int_0^{\frac{2\pi}{\omega}} \int_{x_0}^{x_0+L} \int_0^{2\pi} x^4 \left[R_{21}(u) + R_{22}(v) + R_{23}(w)\right] \sin\frac{m\pi(x - x_0)}{L} \sin(n\theta + \omega t) \sin\alpha d\theta dx dt = 0;\\
&\int_0^{\frac{2\pi}{\omega}} \int_{x_0}^{x_0+L} \int_0^{2\pi} x^4 \left[R_{31}(u) + R_{32}(v) + R_{33}(w)\right] \sin\frac{m\pi(x - x_0)}{L} \cos(n\theta + \omega t) \sin\alpha d\theta dx dt = 0.
\end{aligned} \tag{29}$$

Substituting expressions (28) into Eqs. (15-17) then into Eq. (29), after integrating longer and some rearrangements, we obtain

$$\begin{aligned}
\left(H_{11}^0 + H_{11}^1\omega^2\right)\Psi_1 + \left(H_{12}^0 + H_{12}^1\omega\right)\Psi_2 + H_{13}^0\Psi_3 = 0;\\
\left(H_{21}^0 + H_{21}^1\omega\right)\Psi_1 + \left(H_{22}^0 + H_{22}^1\omega^2\right)\Psi_2 + \left(H_{23}^0 + H_{23}^1\omega\right)\Psi_3 = 0;\\
H_{31}^0\Psi_1 + \left(H_{32}^0 + H_{32}^1\omega\right)\Psi_2 + \left(H_{33}^0 + H_{33}^1\omega^2\right)\Psi_3 = 0;
\end{aligned} \tag{30}$$

where the coefficients H_{ij}^0, H_{ij}^1 are given in Appendix II.

For Eq. (30) to have nontrivial solution, the determinant of the characteristic matrix should be set equal to zero. Developing that determinant and solving resulting equation for frequency ω, yields

$$\begin{aligned}
&H_{11}^1H_{22}^1H_{33}^1\omega^6 + \left[H_{11}^1H_{22}^1H_{33}^0 + H_{11}^0H_{22}^1H_{33}^1 + H_{11}^1H_{22}^0H_{33}^1 - H_{12}^1H_{21}^1H_{33}^1 - H_{11}^1H_{32}^1H_{23}^1\right]\omega^4\\
&- \left[H_{12}^0H_{21}^1H_{33}^1 + H_{12}^1H_{21}^0H_{33}^1 + H_{11}^1H_{32}^1H_{23}^0 + H_{11}^1H_{32}^0H_{23}^1\right]\omega^3\\
&+ \left[H_{11}^0H_{22}^1H_{33}^0 + H_{11}^1H_{22}^0H_{33}^0 + H_{11}^0H_{22}^0H_{33}^1 + H_{13}^0H_{21}^1H_{32}^1 + H_{31}^0H_{23}^1H_{12}^1\right.\\
&\left. - H_{13}^0H_{31}^0H_{22}^1 - H_{12}^1H_{21}^1H_{33}^0 - H_{12}^0H_{21}^0H_{33}^1 - H_{11}^1H_{23}^0H_{32}^0 - H_{11}^0H_{32}^1H_{23}^1\right]\omega^2\\
&+ \left[H_{13}^0H_{21}^0H_{32}^1 + H_{13}^0H_{21}^1H_{32}^0 + H_{23}^0H_{12}^1H_{31}^0 + H_{31}^0H_{23}^1H_{12}^0 - H_{12}^0H_{21}^1H_{33}^0\right.
\end{aligned} \tag{31}$$

$$-H_{12}^{1}H_{21}^{0}H_{33}^{0}-H_{11}^{0}H_{32}^{1}H_{23}^{0}-H_{11}^{0}H_{32}^{0}H_{23}^{1}\Big]\omega+H_{11}^{0}H_{22}^{0}H_{33}^{0}+H_{13}^{0}H_{21}^{0}H_{32}^{0}$$
$$+H_{31}^{0}H_{12}^{0}H_{23}^{0}-H_{13}^{0}H_{31}^{0}H_{22}^{0}-H_{12}^{0}H_{21}^{0}H_{33}^{0}-H_{11}^{0}H_{32}^{0}H_{23}^{0}=0.$$

Eq. (31) is the sixth order polynomial equation for ω and it is used to analyze the frequency characteristics of rotating ES-FGM conical. Numerical results below will show that this equation will have two roots whose absolute values are smallest and they are real numbers, one positive and the other negative. The positive value corresponds to the forward wave and the negative value corresponds to the backward wave.

5 NUMERICAL RESULTS AND DISCUSSION

5.1 Verification of the Present Method

Before stating the analysis of shell frequency characteristics, the validity of the present study should be ensured. Table 1 compares the frequency parameter results of this paper for unstiffened isotropic truncated conical shell with the frequency parameter given by (Hua, 2000)

$$f=\omega R\sqrt{\frac{\rho_{2}}{A_{11}}}$$

Computations have been carried out for a statonary isotropic conical shell with the following data base as:

$$k=0,\ \Omega=0,m=1,\ h/R=0.01,L=0.25R/\sin\alpha,E=4.8265\times10^{9}(Pa),\nu=0.3,\rho=1314\ (\mathrm{kg/m^{3}}).$$

Frequency ω is found from Eq. (31).

It can be observed a good agreement is obtained in this comparison.

f	$\alpha=30^{0}$		$\alpha=45^{0}$		$\alpha=60^{0}$	
N	Present	Hua [14]	Present	Hua [14]	Present	Hua [14]
2	0.8360	0.8420	0.7589	0.7655	0.6322	0.6348
3	0.7365	0.7376	0.7175	0.7212	0.6223	0.6238
4	0.6378	0.6362	0.6725	0.6739	0.6138	0.6145
5	0.5550	0.5528	0.6322	0.6323	0.6106	0.6111
6	0.4962	0.4950	0.6034	0.6035	0.6161	0.6171
7	0.4652	0.4661	0.5908	0.5921	0.6327	0.6350
8	0.4624	0.4660	0.5967	0.6001	0.6618	0.6660
9	0.4854	0.4916	0.6216	0.6273	0.7036	0.7101

Table 1: Comparison of frequency parameter f for a stationary isotropic conical shell with simple-supported boundary conditions.

5.2 ES-FGM Truncated Conical Shells

In the following subsections, the materials used are Alumina with $E_c = 380$ GPa, $\rho_c = 3800\,\text{kg/m}^3$ and Aluminum with $E_m = 70\,\text{GPa}$, $\rho_m = 2702\,\text{kg/m}^3$ and ν=0.3. The stiffeners are FGM.

5.2.1 Effect of Circumferential Wave Number n

Table 2 and Fig. 2a and 2b show effects of circumferential wave number n on frequency ω in case forward wave (Line(a)) and backward wave (Line(b))with volume fraction index k = 1; 5 and semi-vertex angle $\alpha = 30^0; 45^0; 60^0$. Consider stiffeners attached to inside of the shell. The input parameters are taken as h=0.004 m, r/h=30, L/r=2.5, b_1=0.002 m, h_1=0.004 m, n_s=40, b_2=0.002 m, h_2=0.004 m, n_r=40, m=1, Ω=150 rad/s, k=k_2=k_3=1. As can be seen that at the same rotating velocity Ω when $n \le 3$ the frequency ω decreases with the increase of circumferential wave number n. But the frequency ω increases with the increase of circumferential wave number n when $n \ge 5$. We also can be seen that frequency ω has the minimum value at mode (m, n)=(1,4).

ω	a=30^0		a=45^0		a=60^0	
n=1	[(a)]0.2582e+5	-[(b)]0.2564e+5	[(a)]0.1983e+5	-[(b)]0.1974e+5	[(a)]0.1317e+5	-[(b)]0.1314e+5
2	0.1673e+5	-0.1656e+5	0.1400e+5	-0.1389e+5	0.0987e+5	-0.0982e+5
3	0.1156e+5	-0.1143e+5	0.1003e+5	-0.0994e+5	0.0742e+5	-0.0738e+5
4	**0.1044e+5**	**-0.1034e+5**	**0.0868e+5**	**-0.0861e+5**	**0.0674e+5**	**-0.0671e+5**
5	0.1276e+5	-0.1268e+5	0.0989e+5	-0.0983e+5	0.0792e+5	-0.0789e+5
6	0.1720e+5	-0.1714e+5	0.1287e+5	-0.1282e+5	0.1039e+5	-0.1037e+5
7	0.2299e+5	-0.2294e+5	0.1696e+5	-0.1693e+5	0.1371e+5	-0.1370e+5
8	0.2986e+5	-0.2982e+5	0.2191e+5	-0.2188e+5	0.1770e+5	-0.1769e+5
9	0.3773e+5	-0.3769e+5	0.2760e+5	-0.2757e+5	0.2229e+5	-0.2228e+5
10	0.4656e+5	-0.4652e+5	0.3400e+5	-0.3398e+5	0.2745e+5	-0.2744e+5

Forward wave-Line(a), Backward wave-Line(b).

Table 2: Effect of circumferential wave number n on frequency ω.

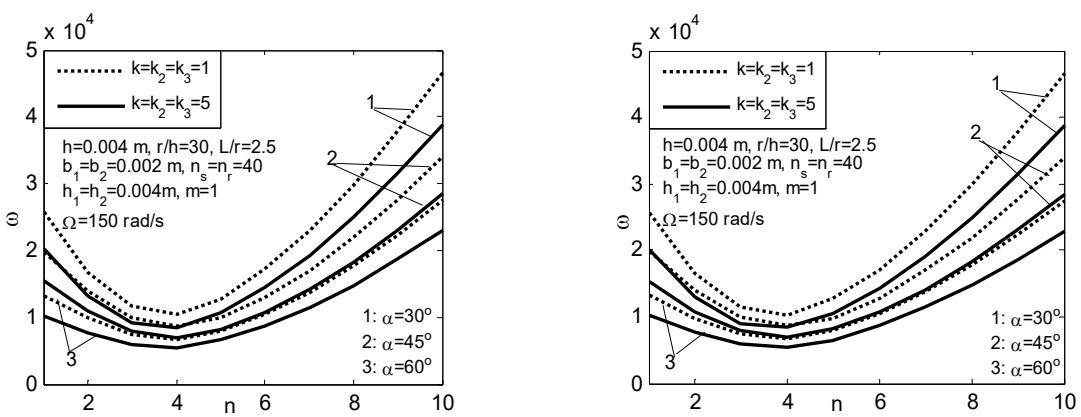

Line (a) - Forward wave

Line (b) - Backward wave

Figure 2: Effects of circumferential wave number n on frequency ω (m=1).

5.2.2 Effect of Rotating Speed Ω

Table 3 describes effects of rotating speed Ω on the critical frequency. It is clear that the critical frequency ω increases with the increase of Ω. For example, in Table 3, for the forward wave (with $\alpha = 60^0$) when the rotating speed Ω varies the values from 0 to 2000 (rad/s), the value ω_{cr} increases from 0.0670e+5 to 0.0970e+5. This increase is considerable about 30.9 %.

Graphically, Figs. 3 and 4 also show that the critical frequency ω increases with the increase of Ω. In addition when the conical shell is a stationary state (for Ω =0) a standing wave occurs. However, forward and backward waves will appear when the conical shell starts to rotate.

ωcr	$\alpha = 15^0$		$\alpha = 30^0$		$\alpha = 45^0$		$\alpha = 60^0$	
Ω=0 rad/s	0.1191e+5 (3)		0.1037 e+5 (4)		0.0863e+5 (4)		0.0670e+5 (4)	
Ω=50 rad/s	0.1194e+5 (3)*	-0.1188e+5 (3)	0.1039e+5 (4)	-0.1036e+5 (4)	0.0864e+5 (4)	-0.0862e+5 (4)	0.0671e+5 (4)	-0.0670e+5 (4)
Ω=100 rad/s	0.1197e+5 (3)	-0.1186e+5 (3)	0.1042e+5 (4)	-0.1035e+5 (4)	0.0866e+5 (4)	-0.0861e+5 (4)	0.0672 e+5 (4)	-0.0670e+5 (4)
Ω=200 rad/s	0.1203e+5 (3)	-0.1181e+5 (3)	0.1047e+5 (4)	-0.1033e+5 (4)	0.0871e+5 (4)	-0.0862e+5 (4)	0.0677e+5 (4)	-0.0672e+5 (4)
Ω=500 rad/s	0.1226e+5 (3)	-0.1171e+5 (3)	0.1072e+5 (4)	-0.1038e+5 (4)	0.0896e+5 (4)	-0.0873e+5 (4)	0.0704e+5 (4)	-0.0693e+5 (4)
Ω=1000 rad/s	0.1277e+5 (3)	-0.1167e+5 (3)	0.1140e+5 (4)	-0.1071e+5 (4)	0.0969e+5 (4)	-0.0923e+5 (4)	0.0789e+5 (4)	-0.0766e+5 (4)
Ω=1500 rad/s	0.1343e+5 (3)	-0.1177e+5 (3)	0.1238e+5 (4)	-0.1134e+5 (4)	0.1075e+5 (4)	-0.1006e+5 (4)	0.0880e+5 (3)	-0.0839e+5 (3)
Ω=2000 rad/s	0.1421e+5 (3)	-0.1201e+5 (3)	0.1358e+5 (4)	-0.1220e+5 (4)	0.1206e+5 (4)	-0.1115e+5 (4)	0.0970e+5 (3)	-0.0916e+5 (3)

* Circumferential wave number n

h=0.004 m, r/h=30, L/r=2.5, b_1=0.002 m, h_1=0.004 m, n_s=40, b_2=0.002 m, h_2=0.004 m, n_r=40, m=1, $k = k_2 = k_3$.

Table 3: Effect of rotating speed Ω on critical frequency ω_{cr} (inside FGM stiffener).

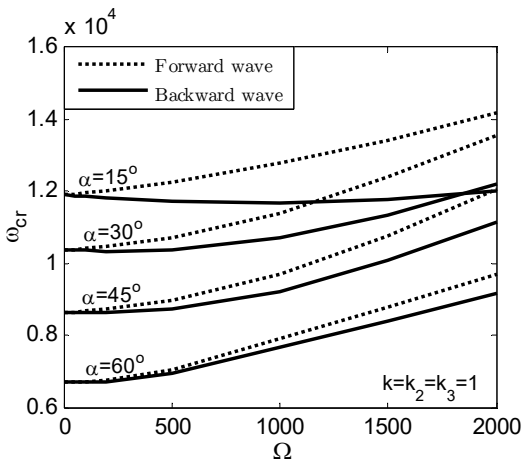

Figure 3: Effects of Ω on critical frequency ω_{cr} (a changes).

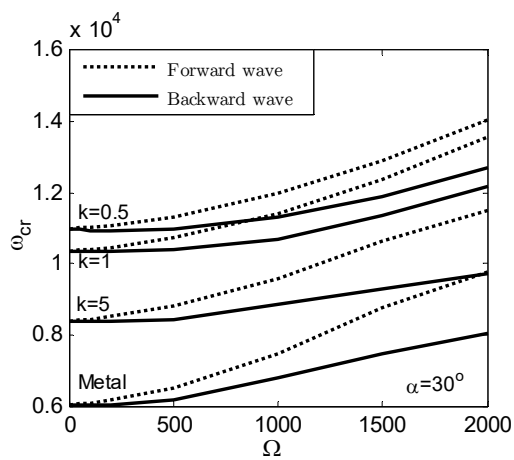

Figure 4: Effects of Ω on critical frequency ω_{cr} (k changes).

5.2.3 Effect of Semi-Vertex Angle α

Table 4 presents effects of semi-vertex angle α on critical frequency ω_{cr}. The geometrical parameters of shell and stiffener are given by h=0.004 m, r/h=30, L/r=2.5, b_1=0.002 m, h_1=0.004 m, n_s=40, b_2=0.002 m, h_2=0.004 m, n_r=40, m=1, Ω=150 rad/s, k2=k3=k.

As can be observed that the critical frequency of shell decreases when the semi-vertex angle increases. This decrease is significant. For example, for the forward wave with Ω=150 rad/s, k=1 when the semi-vertex angle varies the values from 10^0 to 80^0, the critical frequency ω_{cr} decreases from 0.1215e +5 to 0.0342e+5.

Graphically, Fig. 5 also shows that critical frequency decreases when α increases.

ω_{cr}	k=0.5		k=1		k=5	
$\alpha=10^0$	0.1295e+5 (3)	-0.1278e+5 (3)	0.1215e+5 (3)	-0.1198e+5 (3)	0.0974e+5 (3)	-0.0957e+5 (3)
$\alpha=15^0$	0.1283e+5 (3)	-0.1267e+5 (3)	0.1200e+5 (3)	-0.1183e+5 (3)	0.0956e+5 (3)	-0.0940e+5 (3)
$\alpha=20^0$	0.1258e+5 (4)	-0.1245e+5 (4)	0.1192e+5 (3)	-0.1176e+5 (3)	0.0946e+5 (3)	-0.0930e+5 (3)
$\alpha=30^0$	0.1105e+5 (4)	-0.1095e+5 (4)	0.1044e+5 (4)	-0.1034e+5 (4)	0.0848e+5 (4)	-0.0837e+5 (4)
$\alpha=45^0$	0.0922e+5 (4)	-0.0915e+5 (4)	0.0868e+5 (4)	-0.0861e+5 (4)	0.0701e+5 (4)	-0.0694e+5 (4)
$\alpha=60^0$	0.0715e+5 (4)	-0.0712e+5 (4)	0.0674e+5 (4)	-0.0671e+5 (4)	0.0547e+5 (4)	-0.0544e+5 (4)
$\alpha=75^0$	0.0464e+5 (3)	-0.0463e+5 (3)	0.0434e+5 (3)	-0.0433e+5 (3)	0.03505e+5 (3)	-0.03494e+5 (3)
$\alpha=80^0$	0.0364e+5 (3)	-0.0364e+5 (3)	0.0342e+5 (3)	-0.0342e+5 (3)	0.02811e+5 (3)	-0.02807e+5 (3)

Table 4: Effect of semi-vertex angle α on critical frequency ω_{cr} (inside FGM stiffener).

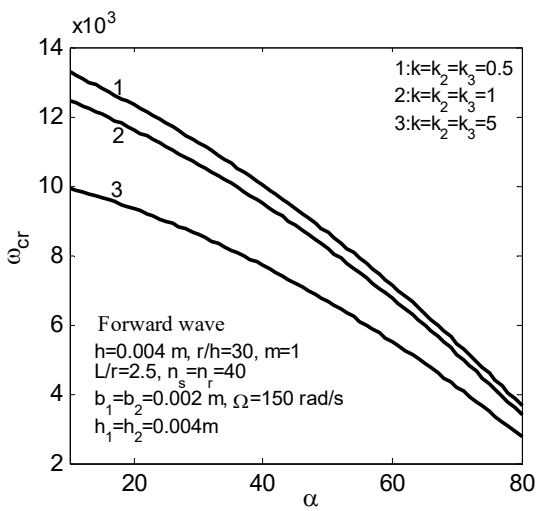

Figure 5: Effects of α on the critical frequency ω_{cr}.

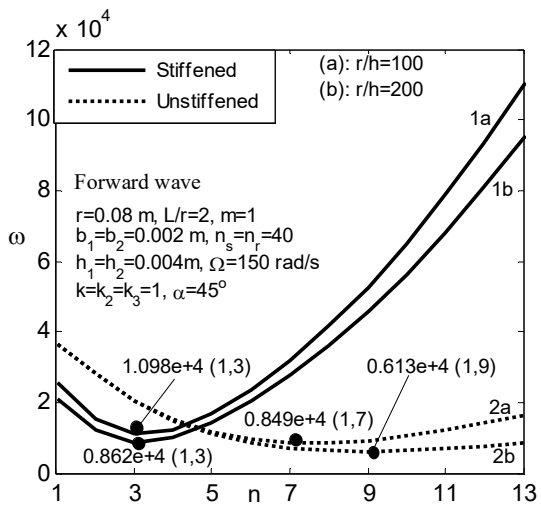

Figure 6a: Effects of stiffeners on frequency ω.

5.2.4 Effect of Stiffeners

Table 5 describes effects of stiffener on frequency with r/h=100, r=0.08 m, L/r=2, b_1=0.002 m, h_1=0.004 m, b_2=0.002 m, h_2=0.004 m, m=1, Ω=150 rad/s, k=k2=k3=1, $a=45^0$. From obtained results as can be seen with the same stiffener numbers, the critical frequency ω_{cr} of orthogonally stiffened shell is the biggest and the critical frequency ω_{cr} of the shell with the stringer is the smallest.

Figs 6 describes effects of stiffener on frequency with two cases r/h=100 and r/h=200. As can be observed the $\omega - n$ curves of stiffened FGM rotating conical shell are lower than those of un-

stiffened FGM rotating conical shell when the value of n is smaller any value n_* (In this example $n_* = 4$) and inverse trend for $n > n_*$.

$\omega\times10^{-5}$	Stringer n_s=80, n_r=0		Ring n_s=0, n_r=80		Orthogonal n_s=40, n_r=40	
n=1	0.2779	-0.2772	0.2253	-0.2236	0.2579	-0.2564
n=2	0.2091	-0.2082	0.1278	-0.1266	0.1550	-0.1539
n=3	0.1527	-0.1518	**0.0915**	**-0.0908**	**0.1098**	**-0.1091**
n=4	0.1135	-0.1127	0.1074	-0.1070	0.1190	-0.1185
n=5	0.0888	-0.0882	0.1565	-0.1562	0.1666	-0.1663
n=6	0.0759	-0.0753	0.2239	-0.2238	0.2352	-0.2350
n=7	**0.0719**	**-0.0715**	0.3055	-0.3055	0.3190	-0.3189
n=8	0.0745	-0.0741	0.4002	-0.4004	0.4164	-0.4165
n=9	0.0814	-0.0810	0.5076	-0.5079	0.5271	-0.5273
n=10	0.0913	-0.0909	0.6274	-0.6278	0.6507	-0.6510

Table 5: Effect of stiffeners on the frequency ω.

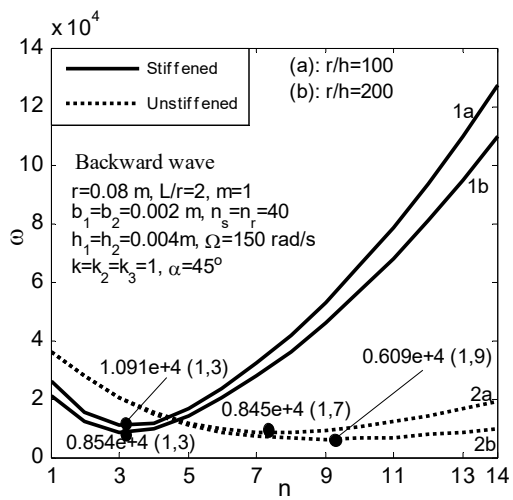

Figure 6b: Effects of stiffeners on the frequency ω.

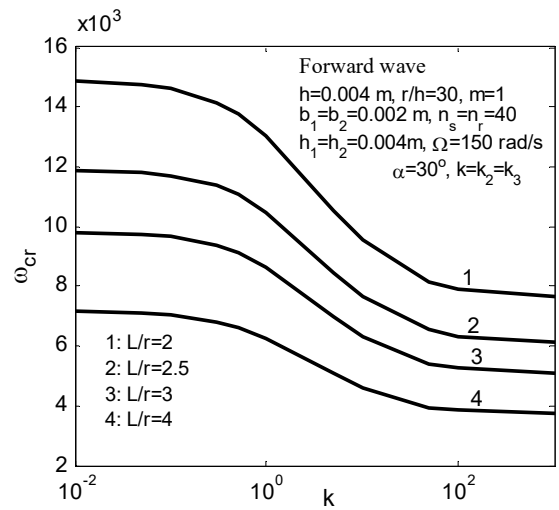

Figure 7: Effects of k on the critical frequency ω_{cr} (L/r changes).

5.2.5 Effect of Volume Fraction Index k

Table 6 considers effects of index volume k on the critical frequency for a stiffened FGM truncated conical shell when the rotating speed Ω=0 rad/s, 150 rad/s and 400 rad/s.

Fig. 7 plots 4 lines $\omega_{cr} - k$ corresponding to L/r=2; 2.5; 3; 4.

Fig.8 plots 4 lines $\omega_{cr} - k$ corresponding to $\alpha = 15^0; 30^0; 45^0; 60^0$.

It is found that the critical frequency ω_{cr} decreases when k increase. This is reasonable because the value increase of k implies the increase of metal constituent in shell. So the stiffness of shell decreases and that leads to the critical frequency ω_{cr} decreases.

ω_{cr}	Ω=0 rad/s	Ω=150 rad/s		Ω=400 rad/s	
Ceramic	0.1185e+5 (4)	0.1192e+5(4)	-0.1182e+5 (4)	0.1209e+5 (4)	-0.1182e+5 (4)
k=0.5	0.1098e+5 (4)	0.1105e+5 (4)	-0.1095e+5 (4)	0.1123e+5 (4)	-0.1095e+5 (4)
k=1	0.1037e+5 (4)	0.1044e+5 (4)	-0.1034e+5 (4)	0.1063e+5 (4)	-0.1035e+5 (4)
k=5	0.0840e+5 (4)	0.0848e+5 (4)	-0.0837e+5 (4)	0.0868e+5 (4)	-0.0840e+5 (4)
k=10	0.0760e+5 (4)	0.0768e+5 (4)	-0.0757e+5 (4)	0.0790e+5 (4)	-0.0762e+5 (4)
Metal	0.0603e+5 (4)	0.0611e+5 (4)	-0.0601e+5 (4)	0.0636e+5 (4)	-0.0609e+5 (4)

h=0.004 m, r/h=30, L/r=2.5, b_1=0.002 m, h_1=0.004 m, n_s=40, b_2=0.002 m, h_2=0.004 m, n_r=40, m=1, $\alpha=30^0$, $k_2=k_3=k$.

Table 6: Effect of volume fraction index k on the critical frequency (inside FGM stiffener).

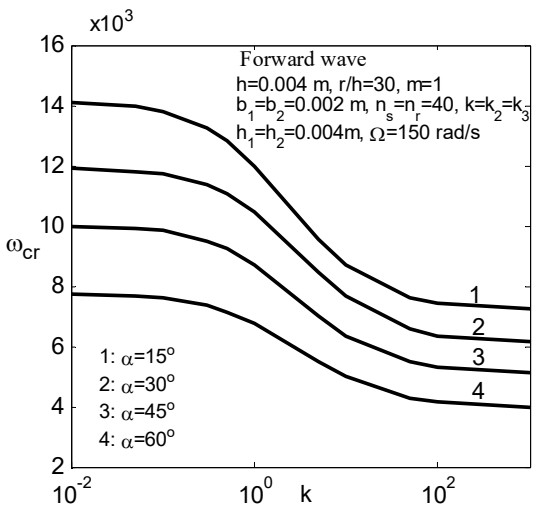

Figure 8: Effects of k on critical frequency ω_{cr} (α changes).

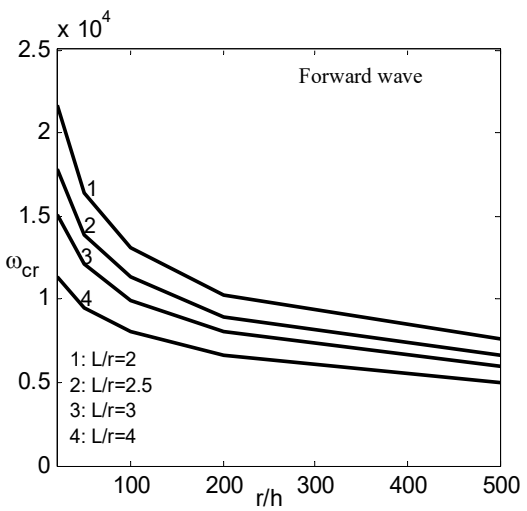

Figure 9: Effects of r/h on the critical frequency ω_{cr}.

5.2.6 Effect of r/h and L/r

Tables 7, 8 and Fig. 9 illustrate effects of the radius-to-thickness ratio r/h and length-to-radius ratio L/r on critical frequency ω_{cr} of stiffened FGM truncated conical shells with the parameters given by r=0.08 m, b_1=0.002 m, h_1=0.004 m, n_s=40, b_2=0.002 m, h_2=0.004 m, n_r=40, m=1, Ω=150 rad/s, $k=k_2=k_3=1$, $\alpha=30^0$.

Figs. 10 and 11 show the effects of r/h ratio and L/r ratio on frequency ω of the shell. It is observed that the critical frequency ω_{cr} as well ω decrease markedly with the increase of those ratios. This decrease is considerable. For example in Table 7, the value ω_{cr} = 0.3775e+5 (with r/h=20, L/r=1) decreases about 1.8 times in comparison with ω_{cr} = 0.2052e+5 (with r/h=100, L/r=1).

ω_{cr}	L/r=1	2	2.5	3	4	5
r/h=20	0.3775e+5 (3)	0.2166e+5 (3)	0.1781 (3)	0.1504e+5 (3)	0.1135e+5 (3)	0.0903e+5 (3)
50	0.2632e+5 (3)	0.1639e+5 (3)	0.1392 (3)	0.1207e+5 (3)	0.0948e+5 (3)	0.0765e+5 (4)
100	0.2052e+5 (3)	0.1307e+5 (3)	0.1130 (3)	0.0997e+5 (3)	0.0805e+5 (3)	0.0673e+5 (3)
200	0.1614e+5 (3)	0.1029e+5 (3)	0.0899 (3)	0.0802e+5 (3)	0.0661e+5 (3)	0.0563e+5 (3)
500	0.1224e+5 (3)	0.0765e+5 (3)	0.0668 (3)	0.0597e+5 (3)	0.0497e+5 (3)	0.0428e+5 (3)

Table 7: Effect of r/h and L/r on the critical frequency ω_{cr} (forward wave).

ω_{cr}	L/r=1	2	2.5	3	4	5
r/h=20	-0.3765e+5 (3)	-0.2153e+5 (3)	-0.1768 (3)	-0.1491e+5 (3)	-0.1121e+5 (3)	-0.0889e+5 (3)
50	-0.2622e+5 (3)	-0.1627e+5 (3)	-0.1380 (3)	-0.1195e+5 (3)	-0.0935e+5 (3)	-0.0754e+5 (4)
100	-0.2041e+5 (3)	-0.1295e+5 (3)	-0.1118 (3)	-0.0984e+5 (3)	-0.0792e+5 (3)	-0.0660e+5 (3)
200	-0.1603e+5 (3)	-0.1017e+5 (3)	-0.0887 (3)	-0.0789e+5 (3)	-0.0649e+5 (3)	-0.0550e+5 (3)
500	-0.1213e+5 (3)	-0.0754e+5 (3)	-0.0656 (3)	-0.0585e+5 (3)	-0.0484e+5 (3)	-0.0415e+5 (3)

Table 8: Effect of r/h and L/r on the critical frequency ω (backward wave).

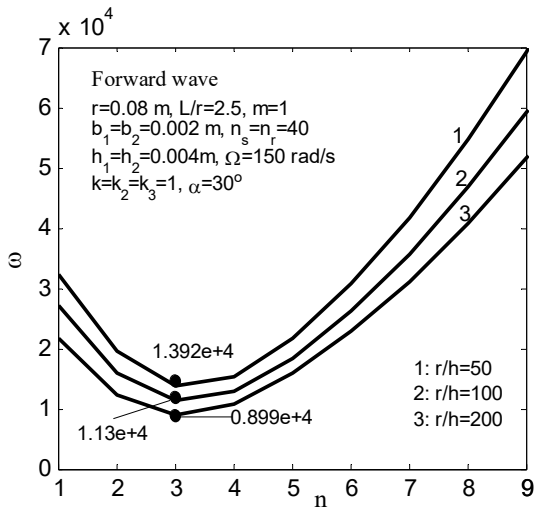

Figure 10: Effects of r/h on the frequency ω

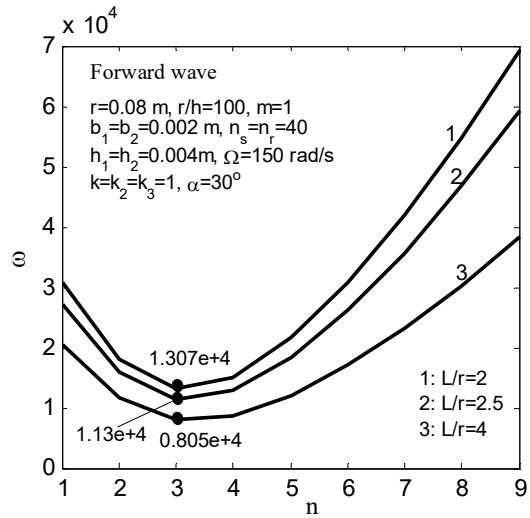

Figure 11: Effects of L/r on the frequency ω.

5.2.7 Comparison Between Outside FGM Stiffener and Inside FGM Stiffener

Table 9 compares effects of outside FGM stiffener and inside FGM stiffener on the critical frequency with k=0.5; 1; 5 and $\alpha=10^0$; 30^0; 45^0; 60^0; 75^0 and h=0.004 m, r/h=30, L/r=2.5, b_1=0.002 m, h_1=0.004 m, n_s=40, b_2=0.002 m, h_2=0.004 m, n_r=40, m=1, Ω=150 rad/s, k_2=k_3=1/k. We can see with the same input parameter the critical frequency ω_{cr} for inside FGM stiffener is bigger than outside FGM stiffener when $10^0 \le \alpha \le 45^0$ while $60^0 \le \alpha \le 75^0$ the critical frequency ω_{cr} for inside FGM stiffener is smaller than outside FGM stiffener.

ω_{cr}	k=0.5		k=1		k=5	
$\alpha=10^0$	[a]0.1246e+5 (3)	-0.1228e+5 (3)	0.1140e+5 (4)	-0.1125e+5 (4)	0.0903e+5 (3)	-0.0885e+5 (3)
	[b]0.1295e+5 (3)	-0.1278e+5 (3)	0.1215e+5 (3)	-0.1198e+5 (3)	0.0974e+5 (3)	-0.0957e+5 (3)
$\alpha=30^0$	[a]0.1045e+5 (4)	-0.1033e+5 (4)	0.0956e+5 (4)	-0.0944e+5 (4)	0.0761e+5 (4)	-0.0749e+5 (4)
	[b]0.1105e+5 (4)	-0.1095e+5 (4)	0.1044e+5 (4)	-0.1034e+5 (4)	0.0848e+5 (4)	-0.0837e+5 (4)
$\alpha=45^0$	[a]0.0919e+5 (4)	-0.0911e+5 (4)	0.0834e+5 (5)	-0.0827e+5 (5)	0.0671e+5 (4)	-0.0663e+5 (4)
	[b]0.0922e+5 (4)	-0.0915e+5 (4)	0.0868e+5 (4)	-0.0861e+5 (4)	0.0701e+5 (4)	-0.0694e+5 (4)
$\alpha=60^0$	[a]0.0728e+5 (4)	-0.0724e+5 (4)	0.0669e+5 (4)	-0.0665e+5 (4)	0.0534e+5 (4)	-0.0530e+5 (4)
	[b]0.0715e+5 (4)	-0.0712e+5 (4)	0.0674e+5 (4)	-0.0671e+5 (4)	0.0547e+5 (4)	-0.0544e+5 (4)
$\alpha=75^0$	[a]0.0505e+5 (4)	-0.0504e+5 (3)	0.0460e+5 (4)	-0.0458e+5 (4)	0.0371e+5 (3)	-0.0370e+5 (3)
	[b]0.0464e+5 (3)	-0.0463e+5 (3)	0.0434e+5 (3)	-0.0433e+5 (3)	0.03505e+5 (3)	-0.03494e+5 (3)

[a] Outside FGM stiffener, [b] Inside FGM stiffener

Table 9: Comparison of critical frequency ω_{cr} between outside FGM stiffener and inside FGM stiffener when the semi-vertex angle a varies.

ω_{cr}	Ω=0 rad/s	Ω=150 rad/s		Ω=400 rad/s	
k=0.5	[a]0.1038e+5 (4)	0.1045e+5 (4)	-0.1033e+5 (4)	0.1064e+5 (4)	-0.1033e+5 (4)
	[b]0.1098e+5 (4)	0.1105e+5 (4)	-0.1095e+5 (4)	0.1123e+5 (4)	-0.1095e+5 (4)
k=1	[a]0.0948e+5 (4)	0.0956e+5 (4)	-0.0944e+5 (4)	0.0976e+5 (4)	-0.0944e+5 (4)
	[b]0.1037e+5 (4)	0.1044e+5 (4)	-0.1034e+5 (4)	0.1063e+5 (4)	-0.1035e+5 (4)
k=5	[a]0.0753e+5 (4)	0.0761e+5 (4)	-0.0749e+5 (4)	0.0784e+5 (4)	-0.0752e+5 (4)
	[b]0.0840e+5 (4)	0.0848e+5 (4)	-0.0837e+5 (4)	0.0868e+5 (4)	-0.0840e+5 (4)
k=10	[a]0.0701e+5 (4)	0.0709e+5 (4)	-0.0697e+5 (4)	0.0733e+5 (4)	-0.0702e+5 (4)
	[b]0.0760e+5 (4)	0.0768e+5 (4)	-0.0757e+5 (4)	0.0790e+5 (4)	-0.0762e+5 (4)

[a] Outside FGM stiffener, [b] Inside FGM stiffener

h=0.004 m, r/h=30, L/r=2.5, b_1=0.002 m, h_1=0.004 m, n_s=40, b_2=0.002 m, h_2=0.004 m, n_r=40, m=1, $\alpha=30^0$, $k_2=k_3=1/k$.

Table 10: Comparison of critical frequency ω_{cr} between outside FGM stiffener and inside FGM stiffener when the volume fraction index k varies.

Table 10 compares effects of inside FGM stiffener and outside FGM stiffener on the critical frequency with k=0.5; 1; 5; 10 and Ω=0; 150; 400 rad/s. As can be seen that the critical frequency ω_{cr} of an inside FGM stiffener attached shell is bigger than one of outside FGM stiffener attached shell.

5.2.8 Comparison Between FGM Stiffener and Homogeneous Stiffener (Inside Stiffener)

Table 11 compares the critical frequencies of homogeneous stiffener attached shell with those of FGM stiffener attached shell when the volume fraction index k=0.5; 1; 5 and α varies the values from 10^o to 60^o.

Table 12 also compares the critical frequencies of homogeneous stiffener attached shell with those of FGM stiffener attached shell when the volume fraction index k=0.5; 1; 5 and the rotating speed Ω=0; 150; 400 (rad/s).

It is found that the critical frequency corresponding to FGM stiffener attached shell is bigger than one of homogeneous stiffener attached shell in these two cases.

ω_{cr}		k=0.5		k=1		k=5	
a=10^0	[a]	0.1173e+5 (4)	-0.1159e+5 (4)	0.1115e+5 (4)	-0.1101e+5 (4)	0.0913e+5 (3)	-0.0896e+5 (3)
	[b]	0.1295e+5 (3)	-0.1278e+5 (3)	0.1215e+5 (3)	-0.1198e+5 (3)	0.0974e+5 (3)	-0.0957e+5 (3)
a=15^0	[a]	0.1100e+5 (4)	-0.1087e+5 (4)	0.1041e+5 (4)	-0.1027e+5 (4)	0.0915e+5 (4)	-0.0902e+5 (4)
	[b]	0.1283e+5 (3)	-0.1267e+5 (3)	0.1200e+5 (3)	-0.1183e+5 (3)	0.0956e+5 (3)	-0.0940e+5 (3)
a=20^0	[a]	0.1055e+5 (4)	-0.1042e+5 (4)	0.0993e+5 (4)	-0.0980e+5 (4)	0.0854e+5 (4)	-0.0841e+5 (4)
	[b]	0.1258e+5 (4)	-0.1245e+5 (4)	0.1192e+5 (3)	-0.1176e+5 (3)	0.0946e+5 (3)	-0.0930e+5 (3)
a=30^0	[a]	0.0992e+5 (4)	-0.0981e+5 (4)	0.0928e+5 (4)	-0.0917e+5 (4)	0.0772e+5 (4)	-0.0761e+5 (4)
	[b]	0.1105e+5 (4)	-0.1095e+5 (4)	0.1044e+5 (4)	-0.1034e+5 (4)	0.0848e+5 (4)	-0.0837e+5 (4)
a=45^0	[a]	0.0839e+5 (5)	-0.0833e+5 (5)	0.0796e+5 (5)	-0.0790e+5 (5)	0.0660e+5 (4)	-0.0652e+5 (4)
	[b]	0.0922e+5 (4)	-0.0915e+5 (4)	0.0868e+5 (4)	-0.0861e+5 (4)	0.0701e+5 (4)	-0.0694e+5 (4)
a=60^0	[a]	0.0673e+5 (4)	-0.0670e+5 (4)	0.0628e+5 (4)	-0.0625e+5 (4)	0.0514e+5 (4)	-0.0511e+5 (4)
	[b]	0.0715e+5 (4)	-0.0712e+5 (4)	0.0674e+5 (4)	-0.0671e+5 (4)	0.0547e+5 (4)	-0.0544e+5 (4)

[a] Homogeneous stiffener, [b] FGM stiffener

h=0.004 m, r/h=30, L/r=2.5, b_1=0.002 m, h_1=0.004 m, n_s=40, b_2=0.002 m, h_2=0.004 m, n_r=40, m=1, Ω=150 rad/s.

Table 11: Effect of semi-vertex angle a on critical frequency ω_{cr}.

ω_{cr}		Ω=0 rad/s	Ω=150 rad/s		Ω=400 rad/s	
k=0.5	[a]	0.0985e+5 (4)	0.0992e+5 (4)	-0.0981e+5 (4)	0.1011e+5 (4)	-0.0982e+5 (4)
	[b]	0.1098e+5 (4)	0.1105e+5 (4)	-0.1095e+5 (4)	0.1123e+5 (4)	-0.1095e+5 (4)
k=1	[a]	0.0921e+5 (4)	0.0928e+5 (4)	-0.0917e+5 (4)	0.0948e+5 (4)	-0.0919e+5 (4)
	[b]	0.1037e+5 (4)	0.1044e+5 (4)	-0.1034e+5 (4)	0.1063e+5 (4)	-0.1035e+5 (4)
k=5	[a]	0.0765 e+5 (4)	0.0772e+5 (4)	-0.0761e+5 (4)	0.0794e+5 (4)	-0.0765e+5 (4)
	[b]	0.0840e+5 (4)	0.0848e+5 (4)	-0.0837e+5 (4)	0.0868e+5 (4)	-0.0840e+5 (4)

[a] Homogeneous stiffener, [b] FGM stiffener

h=0.004 m, r/h=30, L/r=2.5, b_1=0.002 m, h_1=0.004 m, n_s=40, b_2=0.002 m, h_2=0.004 m, n_r=40, m=1, α=30^0.

Table 12: Effect of the volume fraction index k on the critical frequency.

6 CONCLUSIONS

An analytical solution is presented, in this paper, to investigate the free vibration of rotating eccentrically stiffened functionally graded truncated conical. Some new contributions are obtained as follows:

i. FGM truncated conical shells are reinforced by FGM stringers and rings in which a change of spacing between stringer stiffeners is considered;

ii. A centrifugal force and Coriolis acceleration are taken into account.

iii. The sixth order polynomial equation for ω is obtained analytically and it is used to analyze the frequency characteristics of rotating ES-FGM conical shells.

iv. Effects of stiffener, geometrics parameters, cone angle, vibration modes and rotating speed on frequency characteristics of the shell forward and backward wave are discussed in detail.

Acknowledgements

This research is funded by Vietnam National Foundation for Science and Technology Development (NAFOSTED) under Grant No. 107.02-2015.11.

References

Bich, D.H., Dung, D.V., Nam, V.H. (2013). Nonlinear dynamic analysis of eccentrically stiffened imperfect functionally graded doubly curved thin shallow shells. Compos Struct 96: 384-95.

Bich, D.H., Dung, D.V., Nam, V.H., Phuong, N.T. (2013). Nonlinear static and dynamic buckling analysis of imperfect eccentrically stiffened functionally graded circular cylindrical thin shells under axial compression. Int J Mech Sci Compos 74: 190-200.

Bich, D.H., Phuong, N.T., Tung, H.V. (2012). Buckling of functionally graded conical panels under mechanical loads. Compos Struct 94: 1379-84.

Brush,D.O., Almroth, B.O. (1975). Buckling of bars, plates and shells. Mc Graw-Hill, New York.

Chandrasekharan, K., Ramamurti. (1981). Axisymmetric free vibration of laminated conical shell. In Proceedings of Int Symposium on the Mech Behaviour of Structural Media, Ottawa 18-21.

Chandrasekharan, K., Ramamurti. (1982). Asymmetric free vibration of layered conical shells. J Mech Design 104: 453-462.

Chen, Y., Zhao, H.B., Shen, Z.P. (1993). Vibration of high speed rotating shells with calculations for cylindrical shells. J Sound Vib 160: 137-60.

Civalek, O. (2006). An efficient method for free vibration analysis of rotating truncated conical shells. Int J Pressure Vessels Piping 83:1–12.

Crenwelge, O.E., Muster, D. (1969). Free vibration of ring and stringer stiffened conical shells. J Acoust Soc Am 46: 176-85.

Dung, D.V., Hoa, L.K. (2015). Nonlinear torsional buckling and post-buckling of eccentrically stiffened FGM cylindrical shells in thermal environment. Compos Part B. 69: 378-88.

Dung, D.V., Hoa, L.K., Nga, N.T. (2014). On the stability of functionally graded truncated conical shells reinforced by functionally graded stiffeners and surrounded by an elastic medium. Compos Struct 108:77-90.

Dung, D.V., Hoa, L.K., Nga, N.T., Anh, L.T.N. (2013). Instability of eccentrically stiffened functionally graded truncated conical shells under mechanical loads. Compos. Struct 106:104-113.

Dung, D.V., Nam, V.H. (2014). Nonlinear dynamic analysis of eccentrically stiffened functionally graded circular cylindrical thin shells under external pressure and surrounded by an elastic medium. European J Mech A/Solids 46: 42-53.

Hua, L. (2000). Frequency analysis of rotating truncated circular orthotropic conical shells with different boundary conditions". Compos Sci Tech 60: 2945-2955.

Hua, L. (2000). Frequency characteristics of a rotating truncated circular layered conical shell. Compos Struct 50: 59 – 68.

Koizumi, M. (1993). The concept of FGM ceramic trasactions. Funct Gradient Mater 34: 3-10.

Lam, K.Y., Hua, L. (1997). Vibration analysis of rotating truncated circular conical shell. Int J Solids Struct 34(2):183 –1 97.

Lam, K.Y., Hua, L. (1999). Influence of boundary conditions on the frequency characteristics of a rotating truncated circular conical shell. J Sound Vib 223:171 – 195.

Lam, K.Y., Li, H., Ng, T.Y., Chua, C.F. (2002). Generalized differential quadrature method for the free vibration of truncated conical panels. J Sound Vib 251(2): 329-48.

Liew, K.M., Ng, T.Y., Zhao, X. (2005). Free vibration analysis of conical shells via the element-Free kp-Ritz method. J Sound Vib 281: 627–45.

Malekzadeh, P., Heydarpour, Y. (2013). Free vibration analysis of rotating functionally graded truncated conical shells. Compos Struct 97:176 – 88.

Mecitoglu, Z. (1996). Vibration characteristics of a stiffened conical shell. J Sound Vib 197(2):191-206.

Mustaffa, B.A.J., Ali, R. (1987). Free vibration analysis of multisymmetric stiffened shells. Comput Struct 27: 803-10.

Najafizadeh, M.M., Hasani, A., Khazaeinejad, P. (2009). Mechanical stability of functionally graded stiffened cylindrical shells. Appl Math Model 33:1151-57.

Rao, S.S., Reddy, E.S. (1981). Optimum design of stiffened conical shells with natural frequency constraints. Comput Struct 14(1-2):103-10.

Reddy, J.N. (2004.). Mechanics of laminated composite plates and shells: Theory and Analysis, Boca Raton; CRC Press.

Shen, H.S. (2009). Functionally graded materials – Nonlinear analysis of plates and shells. LLC CRC Press.

Shu, C. (1996). An efficient approach for free vibration analysis of conical shells. Int J Mech Sci 38: 935-949.

Shu, C. (1996). Free vibration analysis of composite laminated conical shells by generalized differential quadrature. J Sound Vib 194: 587-604.

Sofiyev, A.H. (2009). The vibration and stability behavior of freely supported FGM conical shells subjected to external pressure. Compos Struct 89: 356-66.

Sofiyev, A.H. (2012). The non-linear vibration of FGM truncated conical shells. Compos Struct 94: 2237-45.

Sofiyev, A.H., Kuruoglu, N., Halilov, H.M. (2010). The vibration and stability of non-homogeneous orthotropic conical shells with clamped edges subjected to uniform external pressures. Appl Math Modelling 34(7): 1807-22.

Srinivasan, RS., Krisnan, P.A. (1989). Dynamic analysis of stiffened conical shell panels. Comput Struct 33(3): 831-37.

Talebitooti, M., Ghayour, M., Ziarei-Rad, S., Talebitooti, R. (2010). Free vibrations of rotating composite conical shells with stringer and ring stiffeners. Arch Appl Mech 80: 201-15.

Torabi, J., Kiani, Y., Eslami, M.R. (2013). Linear thermal buckling analysis of truncated hybrid FGM conical shells. Compos Part B 50: 265-72.

Tornabene, F. (2009). Free vibration analysis of functionally graded conical, cylindrical and annular shell structures with a four-parameter power-law distribution. Comput Methods Appl Mech Engrg 198: 2911-35.

Tornabene, F., Viola, E., Inman, D.J. (2009). 2-D differential quadrature solution for vibration analysis of functionally graded conical, cylindrical and annular shell structures. J Sound Vibr 328: 259-90.

Volmir, A.S. (1972). Nonlinear dynamic of plates and shells. Science Edition (in Russian).

Weingarten, V.I. (1965). Free vibration of ring stiffened conical shells. AIAA J 3: 1475-81.

Xu, C.S., Xia, Z.Q, Chia, C.Y. (1996). Nonlinear theory and vibration analysis of laminated truncated thick conical shells. Int Nonlinear Mech 31(2):139-54.

APPENDIX I

$$A_1 = b_1h_1,\ A_2 = b_2h_2,\ z_1 = \frac{h+h_1}{2},\ z_2 = \frac{h+h_2}{2},\ C_2 = \frac{E_{2r}b_2}{d_2},\ C_1^0 = \frac{E_{2s}b_1}{\lambda_0},\ d_1 = \lambda_0 x,\ d_2 = \frac{L}{n_r},$$

$$\lambda_0 = \frac{2\pi\sin\alpha}{n_s},\ A_{11} = A_{22} = \frac{E_1}{1-\nu^2},\ A_{12} = \frac{\nu E_1}{1-\nu^2},\ A_{66} = \frac{E_1}{2(1+\nu)},\ B_{11} = B_{22} = \frac{E_2}{1-\nu^2};$$

$$B_{12} = \frac{\nu E_2}{1-\nu^2},\ B_{66} = \frac{E_2}{2(1+\nu)},\ D_{11} = D_{22} = \frac{E_3}{1-\nu^2},\ D_{12} = \frac{\nu E_3}{1-\nu^2},\ D_{66} = \frac{E_3}{2(1+\nu)};$$

For shell

$$E_1 = E_m h + E_{cm} h / (k+1),\ E_2 = E_{cm} h^2 \left[1/(k+2) - 1/(2k+2)\right];$$

$$E_3 = E_m h^3 / 12 + E_{cm} h^3 \left[1/(k+3) - 1/(k+2) + 1/(4k+4)\right];\ \rho_1 = \rho_2 + \frac{\rho_3}{x};$$

For inside stiffener

$$E_{1s} = E_m h_1 + E_{cm} \frac{h_1}{k_2+1},\ E_{2s} = -E_m \frac{h_1 h + {h_1}^2}{2} - E_{cm}\left(\frac{{h_1}^2}{k_2+2} + \frac{h_1 h}{2k_2+2}\right);$$

$$E_{3s} = E_m \frac{3h_1 h^2 + 6{h_1}^2 h + 4{h_1}^3}{12} + E_{cm}\left(\frac{{h_1}^3}{k_2+3} + \frac{{h_1}^2 h}{k_2+2} + \frac{h_1 h^2}{4k_2+4}\right);$$

$$E_{1r} = E_m h_2 + E_{cm} \frac{h_2}{k_3+1},\ E_{2r} = -E_m \frac{h_2 h + {h_2}^2}{2} - E_{cm}\left(\frac{{h_2}^2}{k_3+2} + \frac{h_2 h}{2k_3+2}\right);$$

$$E_{3r} = E_m \frac{3h_2 h^2 + 6{h_2}^2 h + 4{h_2}^3}{12} + E_{cm}\left(\frac{{h_2}^3}{k_3+3} + \frac{{h_2}^2 h}{k_3+2} + \frac{h_2 h^2}{4k_3+4}\right);$$

$$\rho_2 = \left(\rho_m + \frac{\rho_c - \rho_m}{k+1}\right)h + \left(\rho_m + \frac{\rho_c - \rho_m}{k_3+1}\right)\frac{A_2}{d_2};\ \rho_3 = \left(\rho_m + \frac{\rho_c - \rho_m}{k_2+1}\right)\frac{A_1}{\lambda_0};$$

For outside stiffener

$$E_s = E_c + E_{mc}\left(\frac{2z-h}{2h_1}\right)^{k_2},\ h/2 \le z \le h/2 + h_1;$$

$$E_r = E_c + E_{mc}\left(\frac{2z-h}{2h_2}\right)^{k_3},\ \ k_2 = k_3 = 1/k,\ \ h/2 \le z \le h/2 + h_2;$$

$$E_{1s} = E_c h_1 + E_{mc} \frac{h_1}{k_2+1},\ E_{2s} = E_c \frac{{h_1}^2 + h_1 h}{2} + E_{mc}\left(\frac{{h_1}^2}{k_2+2} + \frac{h_1 h}{2k_2+2}\right);$$

$$E_{3s} = E_c \frac{3h_1 h^2 + 6h_1^2 h + 4h_1^3}{12} + E_{mc}\left(\frac{h_1^3}{k_2+3} + \frac{h_1^2 h}{k_2+2} + \frac{h_1 h^2}{4k_2+4}\right);$$

$$E_{1r} = E_c h_2 + E_{mc} \frac{h_2}{k_3+1},\ E_{2r} = E_c \frac{{h_2}^2 + h_2 h}{2} + E_{mc}\left(\frac{{h_2}^2}{k_3+2} + \frac{h_2 h}{2k_3+2}\right);$$

$$E_{3r} = E_c \frac{3h_2 h^2 + 6h_2^2 h + 4h_2^3}{12} + E_{mc}\left(\frac{h_2^3}{k_3+3} + \frac{h_2^2 h}{k_3+2} + \frac{h_2 h^2}{4k_3+4}\right);$$

$$\rho_2 = \left(\rho_m + \frac{\rho_c - \rho_m}{k+1}\right)h + \left(\rho_c + \frac{\rho_m - \rho_c}{k_3+1}\right)\frac{A_2}{d_2};\ \rho_3 = \left(\rho_c + \frac{\rho_m - \rho_c}{k_2+1}\right)\frac{A_1}{\lambda_0};$$

in which n_s, n_r is the number of stringer and ring stiffener; h_1 and b_1 are the thickness and width of stringer (x-direction); h_2 and b_2 are the thickness and width of ring (θ-direction). Also,

$d_1 = d_1(x)$ and d_2 are the distance between two stringers and two rings, respectively. The quantities z_1, z_2 represent the eccentricities of stiffeners with respect to the middle surface of shell (Fig. 1).

APPENDIX II

$$H_{11}^0 = -\frac{m^2\pi^4}{L^2}A_{11}\sin\alpha\left[\frac{(x_0+L)^4-x_0^4}{4}+\frac{3L^3(2x_0+L)}{4m^2\pi^2}\right]-\frac{m^2\pi^4}{L^2}\frac{E_{1s}b_1}{\lambda_0}\sin\alpha\times\left[\frac{(x_0+L)^3-x_0^3}{3}+\frac{L^3}{2m^2\pi^2}\right]-\frac{n^2\pi^2}{2}\frac{A_{66}}{\sin\alpha}L(2x_0+L)-n^2\pi^2\rho_2\Omega^2\sin\alpha\left[\frac{(x_0+L)^4-x_0^4}{4}+\frac{3L^3(2x_0+L)}{4m^2\pi^2}\right]-n^2\pi^2\rho_3\Omega^2\sin\alpha\left[\frac{(x_0+L)^3-x_0^3}{3}+\frac{L^3}{2m^2\pi^2}\right]-\frac{\pi^2}{2}\left(A_{22}+\frac{E_{1r}b_2}{d_2}\right)\sin\alpha\times L(2x_0+L)+\frac{\pi^2}{2}A_{11}\sin\alpha L(2x_0+L);$$

$$H_{11}^1 = \pi^2\rho_2\sin\alpha\left[\frac{(x_0+L)^4-x_0^4}{4}+\frac{3L^3(2x_0+L)}{4m^2\pi^2}\right]+\pi^2\rho_3\sin\alpha\left[\frac{(x_0+L)^3-x_0^3}{3}+\frac{L^3}{2m^2\pi^2}\right];$$

$$H_{12}^0 = \frac{mn\pi^3}{L}(A_{12}+A_{66})\left[\frac{(x_0+L)^3-x_0^3}{3}+\frac{L^3}{2m^2\pi^2}\right]+\frac{mn\pi^3}{2}\cot\alpha\ (B_{12}+2B_{66})(2x_0+L)+\frac{n\pi L^2}{2m}\left(A_{22}+\frac{E_{1r}b_2}{d_2}+A_{66}\right);$$

$$H_{12}^1 = 2\pi^2\rho_2\Omega\sin^2\alpha\left[\frac{L}{2m\pi}[x_0^3-(x_0+L)^3]+\frac{3L^4}{4m^3\pi^3}\right]-\frac{\pi\rho_3\Omega}{m}\sin^2\alpha\ L^2(2x_0+L);$$

$$H_{13}^0 = \frac{m^3\pi^5}{L^3}B_{11}\sin\alpha\left[\frac{(x_0+L)^4-x_0^4}{4}+\frac{3L^3(2x_0+L)}{4m^2\pi^2}\right]+\frac{m^3\pi^5}{L^3}C_1^0\sin\alpha\left[\frac{(x_0+L)^3-x_0^3}{3}+\frac{L^3}{2m^2\pi^2}\right]+\frac{mn^2\pi^3}{2}\frac{B_{12}+2B_{66}}{\sin\alpha}(2x_0+L)+\frac{m\pi^3}{L}A_{12}\cos\alpha\left[\frac{(x_0+L)^3-x_0^3}{3}+\frac{L^3}{2m^2\pi^2}\right]+\frac{m\pi^3}{2}(B_{22}+C_2)\sin\alpha(2x_0+L)-\frac{m\pi^3}{L}\rho_2\Omega^2\sin^2\alpha\cos\alpha\left[\frac{(x_0+L)^5-x_0^5}{5}-\frac{L^2[x_0^3-(x_0+L)^3]}{m^2\pi^2}-\frac{3L^5}{2m^4\pi^4}\right]-\frac{m\pi^3}{L}\rho_3\Omega^2\sin^2\alpha\cos\alpha\left[\frac{(x_0+L)^4-x_0^4}{4}+\frac{3L^3(2x_0+L)}{4m^2\pi^2}\right]-\frac{m\pi^3}{2}B_{11}\sin\alpha(2x_0+L)+\frac{\pi L^2}{2m}\cos\alpha\left(A_{22}+\frac{E_{1r}b_2}{d_2}\right);$$

$$H_{21}^0 = \frac{mn\pi^3}{L}(A_{12}+A_{66})\left[\frac{(x_0+L)^4-x_0^4}{4}-\frac{3L^3(2x_0+L)}{4m^2\pi^2}\right]+\frac{mn\pi^3}{L}(B_{12}+B_{66})\cot\alpha$$

$$\times\left[\frac{(x_0+L)^3-x_0^3}{3}-\frac{L^3}{2m^2\pi^2}\right]+\frac{mn\pi^3}{L}\rho_2\Omega^2\sin^2\alpha\ \left[\frac{(x_0+L)^6-x_0^6}{6}+\frac{5L^2[x_0^4-(x_0+L)^4]}{4m^2\pi^2}\right.$$

$$\left.+\frac{15L^5(2x_0+L)}{4m^4\pi^4}\right]+\frac{mn\pi^3}{L}\ \rho_3\Omega^2\sin^2\alpha\ \left[\frac{(x_0+L)^5-x_0^5}{5}+\frac{L^2(x_0^3-(x_0+L)^3)}{m^2\pi^2}+\frac{3L^5}{2m^4\pi^4}\right]+\frac{n\pi}{2m}$$

$$\left(A_{22}+\frac{E_{1r}b_2}{d_2}+A_{66}\right)\ L^2(2x_0+L)+\frac{\pi nL^2}{2m}\cot\alpha\ (B_{22}+C_2-B_{66})-n\pi^2\rho_2\Omega^2\ \sin^2\alpha$$

$$\times\left[\frac{L[x_0^4-(x_0+L)^4]}{2m\pi}+\frac{3L^4(2x_0+L)}{2m^3\pi^3}\right]-n\pi^2\rho_3\Omega^2\ \sin^2\alpha\ \left[\frac{L[x_0^3-(x_0+L)^3]}{2m\pi}+\frac{3L^4}{4m^3\pi^3}\right];$$

$$H_{21}^1=2\pi^2\rho_2\Omega\sin^2\alpha\ \left[\frac{L[x_0^4-(x_0+L)^4]}{2m\pi}+\frac{3L^4(2x_0+L)}{2m^3\pi^3}\right]+2\pi^2\rho_3\Omega\sin^2\alpha\times\left[\frac{L[x_0^3-(x_0+L)^3]}{2m\pi}\right.$$

$$\left.+\frac{3L^4}{4m^3\pi^3}\right];$$

$$H_{22}^0=-\frac{m^2\pi^4}{L^2}A_{66}\sin\alpha\ \left[\frac{(x_0+L)^5-x_0^5}{5}+\frac{L^2[x_0^3-(x_0+L)^3]}{m^2\pi^2}+\frac{3L^5}{2m^4\pi^4}\right]-\frac{3m^2\pi^4}{L^2}B_{66}\cos\alpha$$

$$\times\left[\frac{(x_0+L)^4-x_0^4}{4}-\frac{3L^3(2x_0+L)}{4m^2\pi^2}\right]-\frac{2m^2\pi^4}{L^2}D_{66}\cot^2\alpha\sin\alpha\ \left[\frac{(x_0+L)^3-x_0^3}{3}-\frac{L^3}{2m^2\pi^2}\right]-\frac{n^2\pi^2}{\sin\alpha}$$

$$\left(A_{22}+\frac{E_{1r}b_2}{d_2}\right)\left[\frac{(x_0+L)^3-x_0^3}{3}-\frac{L^3}{2m^2\pi^2}\right]-\frac{n^2\pi^2\cot\alpha}{\sin\alpha}\ (B_{22}+C_2)L(2x_0+L)-\frac{n^2\pi^2L\cot^2\alpha}{\sin\alpha}$$

$$\left(D_{22}+\frac{E_{3r}b_2}{d_2}\right)-\pi^2A_{66}\sin\alpha\ \left[\frac{(x_0+L)^3-x_0^3}{3}-\frac{L^3}{2m^2\pi^2}\right]+\frac{\pi^2}{2}B_{66}\times\cos\alpha L(2x_0+L)+6\pi^2LD_{66}$$

$$\times\cot^2\alpha\sin\alpha+\frac{m\pi^3}{L}A_{66}\sin\alpha\ \left[\frac{L[x_0^3-(x_0+L)^3]}{2m\pi}+\frac{3L^4}{4m^3\pi^3}\right]+\frac{\pi^2}{2}B_{66}\cos\alpha\ \ L(2x_0+L)$$

$$+\frac{m\pi^3}{L}\rho_2\Omega^2\sin^3\alpha\ \left[\frac{L[x_0^5-(x_0+L)^5]}{2m\pi}-\frac{5L^3[x_0^3-(x_0+L)^3]}{2m^3\pi^3}-\frac{15L^6}{4m^5\pi^5}\right]+\frac{m\pi^3}{L}\ \rho_3\Omega^2\sin^3\alpha$$

$$\left[\frac{L[x_0^4-(x_0+L)^4]}{2m\pi}+\frac{3L^4(2x_0+L)}{2m^3\pi^3}\right];$$

$$H_{22}^1=\pi^2\rho_2\sin\alpha\ \left[\frac{(x_0+L)^5-x_0^5}{5}+\frac{L^2[x_0^3-(x_0+L)^3]}{m^2\pi^2}+\frac{3L^5}{2m^4\pi^4}\right]+\pi^2\rho_3\sin\alpha\times\left[\frac{(x_0+L)^4-x_0^4}{4}\right.$$

$$\left.-\frac{3L^3(2x_0+L)}{4m^2\pi^2}\right];$$

$$H_{23}^0=-\frac{m^2n\pi^4}{L^2}(B_{12}+2B_{66})\ \left[\frac{(x_0+L)^4-x_0^4}{4}-\frac{3L^3(2x_0+L)}{4m^2\pi^2}\right]-\frac{m^2n\pi^4}{L^2}\cot\alpha\ \ (D_{12}+2D_{66})$$

$$\times\left[\frac{(x_0+L)^3-x_0^3}{3}-\frac{L^3}{2m^2\pi^2}\right]-\frac{n^3\pi^2}{2}\frac{B_{22}+C_2}{\sin^2\alpha}\ \ L(2x_0+L)-\frac{n^3\pi^2L\cot\alpha}{\sin^2\alpha}\ \left(D_{22}+\frac{E_{3r}b_2}{d_2}\right)$$

$$-n\pi^2\cot\alpha\ \left(A_{22}+\frac{E_{1r}b_2}{d_2}\right)\left[\frac{(x_0+L)^3-x_0^3}{3}-\frac{L^3}{2m^2\pi^2}\right]+4n\pi^2LD_{66}\cot\alpha-\frac{n\pi^2}{2}\cot^2\alpha\times(B_{22}+C_2)$$

$$L(2x_0+L)+\frac{n\pi^2L}{2}\cot\alpha\ \left(4D_{66}-D_{22}-\frac{E_{3r}b_2}{d_2}\right)-\frac{n\pi^2}{2}(B_{22}+C_2)\ \ L(2x_0+L);$$

$$H_{23}^1=\pi^2\rho_2\Omega\sin(2\alpha)\ \left[\frac{(x_0+L)^5-x_0^5}{5}+\frac{L^2[x_0^3-(x_0+L)^3]}{m^2\pi^2}+\frac{3L^5}{2m^4\pi^4}\right]+\pi^2\rho_3\Omega\sin(2\alpha)$$

$$\times\left[\frac{(x_0+L)^4-x_0^4}{4}-\frac{3L^3(2x_0+L)}{4m^2\pi^2}\right];$$

$$H_{31}^0=\frac{m^3\pi^5}{L^3}B_{11}\sin\alpha\ \left[\frac{(x_0+L)^5-x_0^5}{5}+\frac{L^2[x_0^3-(x_0+L)^3]}{m^2\pi^2}+\frac{3L^5}{2m^4\pi^4}\right]+\frac{m^3\pi^5}{L^3}C_1^0\sin\alpha$$

$$\times\left[\frac{(x_0+L)^4-x_0^4}{4}-\frac{3L^3(2x_0+L)}{4m^2\pi^2}\right]+\frac{mn^2\pi^3}{L}\ \frac{B_{12}+2B_{66}}{\sin\alpha}\ \left[\frac{(x_0+L)^3-x_0^3}{3}-\frac{L^3}{2m^2\pi^2}\right]$$

$$+\frac{m\pi^3}{L}\ A_{12}\cos\alpha\ \left[\frac{(x_0+L)^4-x_0^4}{4}-\frac{3L^3(2x_0+L)}{4m^2\pi^2}\right]+\frac{m\pi^3}{L}\ (B_{22}+C_2)\sin\alpha\left[\frac{(x_0+L)^3-x_0^3}{3}\right.$$

$$\left.-\frac{L^3}{2m^2\pi^2}\right]+\frac{m\pi^3}{L}\rho_2\Omega^2\ \sin^2\alpha\cos\alpha\ \left[\frac{(x_0+L)^6-x_0^6}{6}+\frac{5L^2[x_0^4-(x_0+L)^4]}{4m^2\pi^2}+\frac{15L^5(2x_0+L)}{4m^4\pi^4}\right]$$

$$+\frac{m\pi^3}{L}\rho_3\Omega^2\ \sin^2\alpha\cos\alpha\ \left[\frac{(x_0+L)^5-x_0^5}{5}+\frac{L^2[x_0^3-(x_0+L)^3]}{m^2\pi^2}+\frac{3L^5}{2m^4\pi^4}\right]-\frac{2m^2\pi^4}{L^2}B_{11}\sin\alpha$$

$$\left[\frac{L[x_0^3-(x_0+L)^3]}{2m\pi}+\frac{3L^4}{4m^3\pi^3}\right]+\frac{\pi n^2L^2}{2m}\ \frac{B_{22}+C_2-2B_{66}}{\sin\alpha}-\frac{\pi L^2}{2m}(B_{22}+C_2)\sin\alpha+\frac{\pi L^2(2x_0+L)}{2m}$$

$$\cos\alpha\left(A_{22}+\frac{E_{1r}b_2}{d_2}\right)+\pi^2\rho_2\Omega^2\ \sin^2\alpha\cos\alpha\times\left[\frac{L[x_0^4-(x_0+L)^4]}{2m\pi}+\frac{3L^4(2x_0+L)}{2m^3\pi^3}\right]+\pi^2\rho_3\Omega^2\ \sin^2\alpha\cos\alpha$$

$$\left[\frac{L[x_0^3-(x_0+L)^3]}{2m\pi}+\frac{3L^4}{4m^3\pi^3}\right];$$

$$H_{32}^0=-\frac{m^2n\pi^4}{L^2}(B_{12}+2B_{66})\ \left[\frac{(x_0+L)^4-x_0^4}{4}-\frac{3L^3(2x_0+L)}{4m^2\pi^2}\right]-\frac{m^2n\pi^4}{L^2}\ (D_{12}+4D_{66})\ \cot\alpha$$

$$\times\left[\frac{(x_0+L)^3-x_0^3}{3}-\frac{L^3}{2m^2\pi^2}\right]-\frac{n^3\pi^2}{2}\ \frac{B_{22}+C_2}{\sin^2\alpha}\ L(2x_0+L)-n^3\pi^2L\ \frac{\cot\alpha}{\sin^2\alpha}\ \left(D_{22}+\frac{E_{3r}b_2}{d_2}\right)+2\pi^2nL$$

$$\cot\alpha\ \left(D_{12}+4D_{66}+D_{22}+\frac{E_{3r}b_2}{d_2}\right)+\frac{n\pi^2}{2}(1-\cot^2\alpha)\ (B_{22}+C_2)\ L(2x_0+L)+n\pi^2B_{66}\ \ L(2x_0+L)$$

$$-n\pi^2\cot\alpha\ \left(A_{22}+\frac{E_{1r}b_2}{d_2}\right)\left[\frac{(x_0+L)^3-x_0^3}{3}-\frac{L^3}{2m^2\pi^2}\right]+\frac{n\pi^2L}{2}\cot\alpha\times\left[2(D_{12}+4D_{66})+D_{22}+\frac{E_{3r}b_2}{d_2}\right]$$

$$+\frac{n\pi^2}{2}\ (B_{22}+C_2+2B_{66})\ \ L(2x_0+L);$$

$$H_{32}^{1} = \pi^2\rho_2\Omega\sin(2\alpha)\left[\frac{(x_0+L)^5-x_0^5}{5}+\frac{L^2[x_0^3-(x_0+L)^3]}{m^2\pi^2}+\frac{3L^5}{2m^4\pi^4}\right]+\pi^2\rho_3\Omega\sin(2\alpha)$$
$$\times\left[\frac{(x_0+L)^4-x_0^4}{4}-\frac{3L^3(2x_0+L)}{4m^2\pi^2}\right];$$

$$H_{33}^{0} = -\frac{m^4\pi^6}{L^4}D_{11}\sin\alpha\left[\frac{(x_0+L)^5-x_0^5}{5}+\frac{L^2[x_0^3-(x_0+L)^3]}{m^2\pi^2}+\frac{3L^5}{2m^4\pi^4}\right]-\frac{m^4\pi^6}{L^4}\frac{E_{3s}b_1}{\lambda_0}\sin\alpha$$
$$\times\left[\frac{(x_0+L)^4-x_0^4}{4}-\frac{3L^3(2x_0+L)}{4m^2\pi^2}\right]-n^4\pi^2\ \frac{L}{\sin^3\alpha}\left(D_{22}+\frac{E_{3r}b_2}{d_2}\right)-\frac{2m^2n^2\pi^4}{L^2}\ \frac{D_{12}+2D_{66}}{\sin\alpha}$$
$$\times\left[\frac{(x_0+L)^3-x_0^3}{3}-\frac{L^3}{2m^2\pi^2}\right]-\frac{2m^2\pi^4}{L^2}\ B_{12}\cos\alpha\left[\frac{(x_0+L)^4-x_0^4}{4}-\frac{3L^3(2x_0+L)}{4m^2\pi^2}\right]-\frac{m^2\pi^4}{L^2}\times\sin\alpha$$
$$\left(D_{22}+\frac{E_{3r}b_2}{d_2}\right)\left[\frac{(x_0+L)^3-x_0^3}{3}-\frac{L^3}{2m^2\pi^2}\right]-n^2\pi^2\frac{\cot\alpha}{\sin\alpha}\ (B_{22}+C_2)\ L(2x_0+L)+\frac{2n^2\pi^2L}{\sin\alpha}$$
$$\left(D_{12}+4D_{66}+D_{22}+\frac{E_{3r}b_2}{d_2}\right)-n^2\pi^2\rho_2\Omega^2\sin\alpha\left[\frac{(x_0+L)^5-x_0^5}{5}+\frac{L^2[x_0^3-(x_0+L)^3]}{m^2\pi^2}+\frac{3L^5}{2m^4\pi^4}\right]$$
$$-n^2\pi^2\rho_3\Omega^2\sin\alpha\left[\frac{(x_0+L)^4-x_0^4}{4}-\frac{3L^3(2x_0+L)}{4m^2\pi^2}\right]+\frac{\pi^2}{2}\cos\alpha(B_{22}+C_2)\ L(2x_0+L)+\pi^2\rho_2\Omega^2$$
$$\cos^2\alpha\sin\alpha\left[\frac{(x_0+L)^5-x_0^5}{5}+\frac{L^2[x_0^3-(x_0+L)^3]}{m^2\pi^2}+\frac{3L^5}{2m^4\pi^4}\right]+\pi^2\rho_3\Omega^2\ \cos^2\alpha\sin\alpha\times\left[\frac{(x_0+L)^4-x_0^4}{4}\right.$$
$$\left.-\frac{3L^3(2x_0+L)}{4m^2\pi^2}\right]-\pi^2\left(A_{22}+\frac{E_{1r}b_2}{d_2}\right)\cot^2\alpha\sin\alpha\left[\frac{(x_0+L)^3-x_0^3}{3}-\frac{L^3}{2m^2\pi^2}\right]+n^2\pi^2L\ \frac{D_{12}+4D_{66}}{\sin\alpha}$$
$$+\frac{\pi^2L}{2}\sin\alpha\times\left(D_{22}+\frac{E_{3r}b_2}{d_2}\right)+\frac{2m^3\pi^5}{L^3}\ D_{11}\ \sin\alpha\left[\frac{L}{2m\pi}\ [x_0^3-(x_0+L)^3]+\frac{3L^4}{4m^3\pi^3}\right];$$

$$H_{33}^{1} = \pi^2\rho_2\sin\alpha\left[\frac{(x_0+L)^5-x_0^5}{5}+\frac{L^2[x_0^3-(x_0+L)^3]}{m^2\pi^2}+\frac{3L^5}{2m^4\pi^4}\right]+\pi^2\rho_3\sin\alpha\times\left[\frac{(x_0+L)^4-x_0^4}{4}\right.$$
$$\left.-\frac{3L^3(2x_0+L)}{4m^2\pi^2}\right].$$